Distance Measurements in Magic-Angle Spinning Solid-State NMR

Prof. Mei Hong
Department of Chemistry
Massachusetts Institute of Technology

Pre-ISMAR NMR Workshop, Moreton Bay Research Station, North Stradbroke Island, Univ. Queensland, Brisbane, Australia, August 18-20, 2023

Outline

- Homonuclear distances from 2D isotropic spin exchange
- Homonuclear distances from anisotropic spin exchange (CODEX)
- Heteronuclear distances from REDOR
- These techniques are illustrated using the ^{19}F spin
- Examples of applications to membrane proteins and amyloid proteins

Distance Measurements in Solid-State NMR

^{19}F

- ✓ Is 100% abundant
- ✓ Has no background in biomolecules
- ✓ Can be readily incorporated
- ✓ Has large chemical shifts
- ✓ Is a good distance probe, $\gamma_F = 94\% \ \gamma_H$

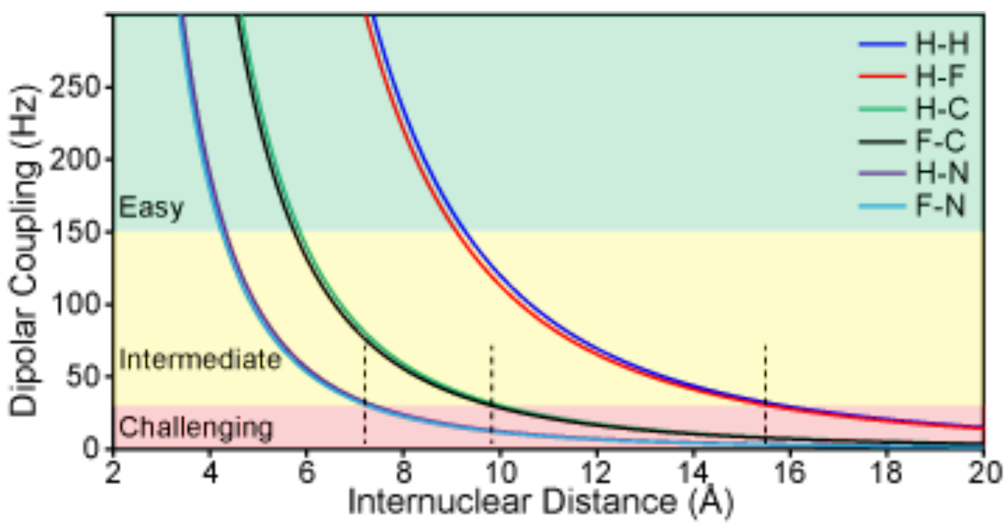

Shcherbakov et al. ***Chem. Reviews***, 2022.

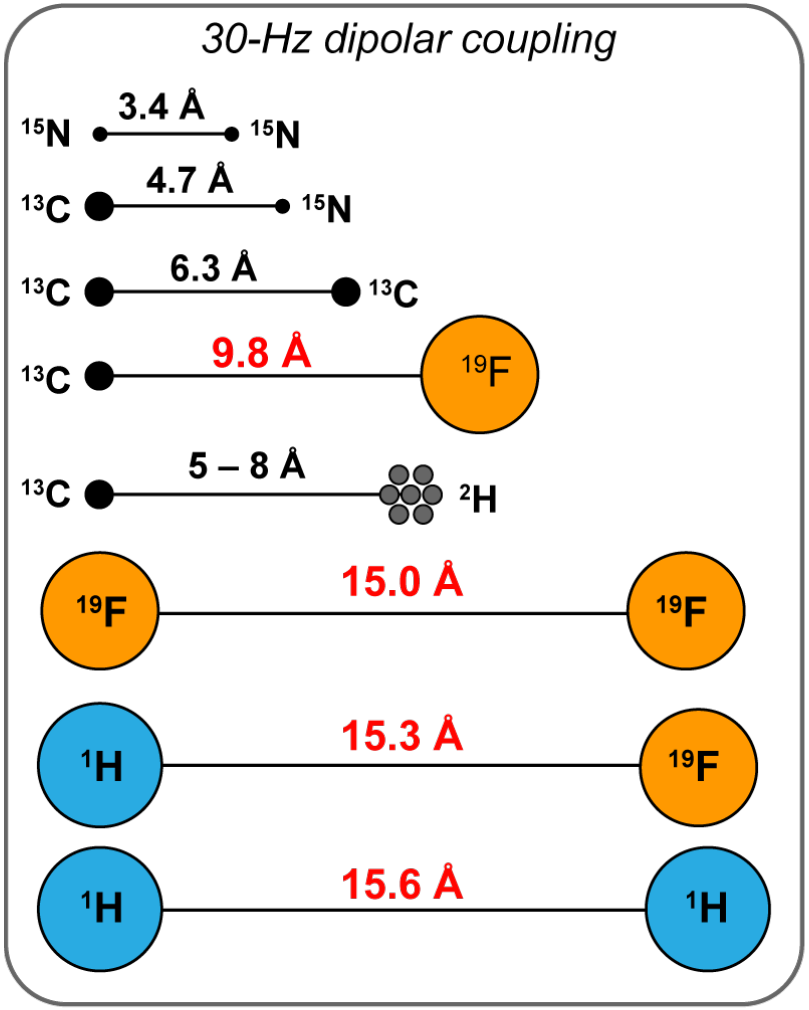

^{19}F NMR: Gronenborn, Arthanari, Prosser, Wuthrich, Schaefer, Polenova, McDermott, Rienstra, Emsley, Su

Fluorines in Chemistry and Biology

~30% of medicinal compounds contain ^{19}F

Synthetic peptides:
- Site-specific fluorination

Recombinant proteins:
- glyphosate

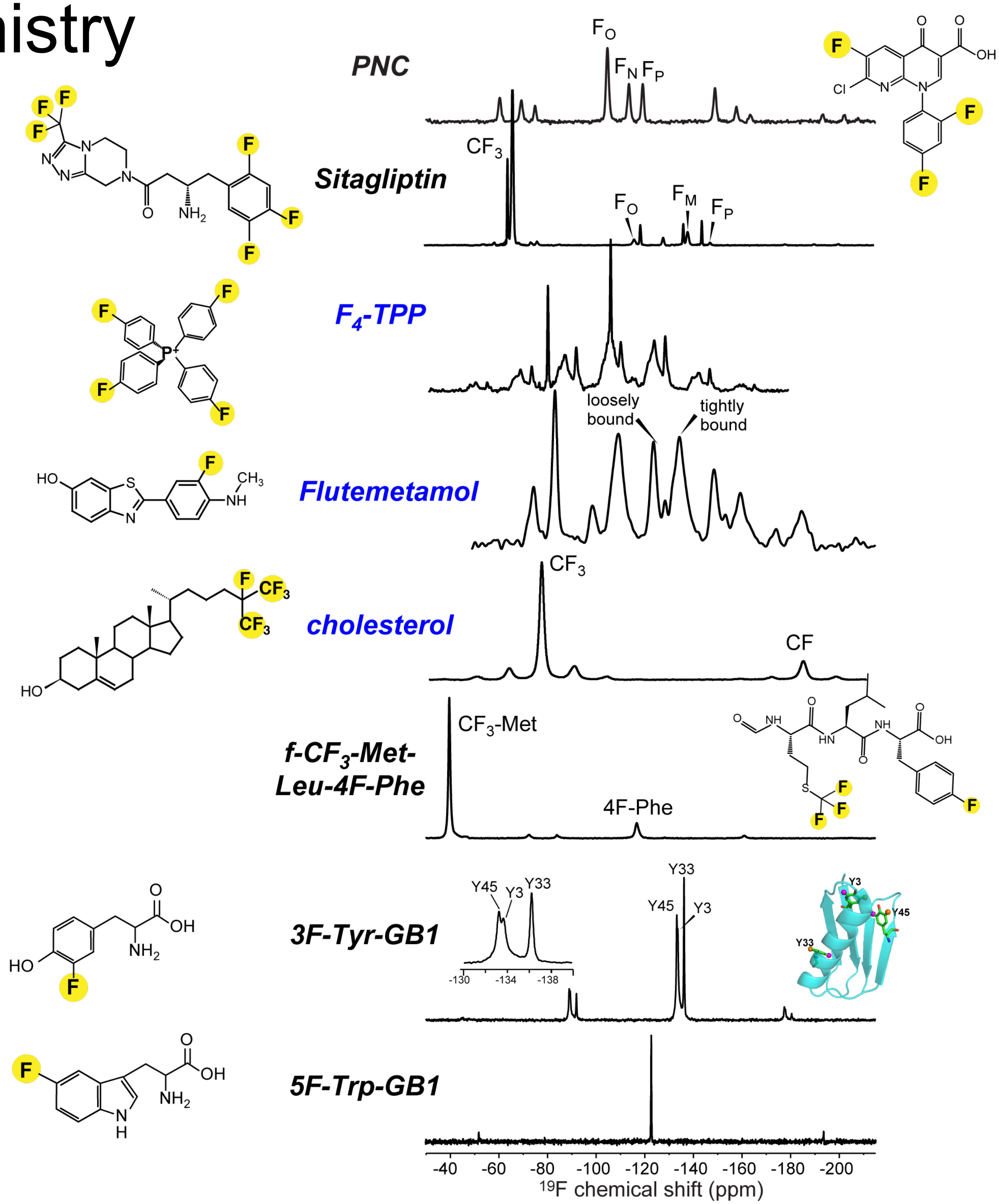

Homonuclear 2D ^{19}F-^{19}F Spin Exchange for Chemically Inequivalent Spins (Isotropic Spin Exchange)

Spectrally Resolved ^{19}F Spin Exchange

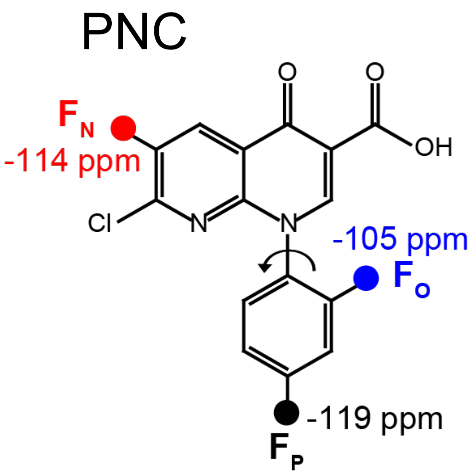

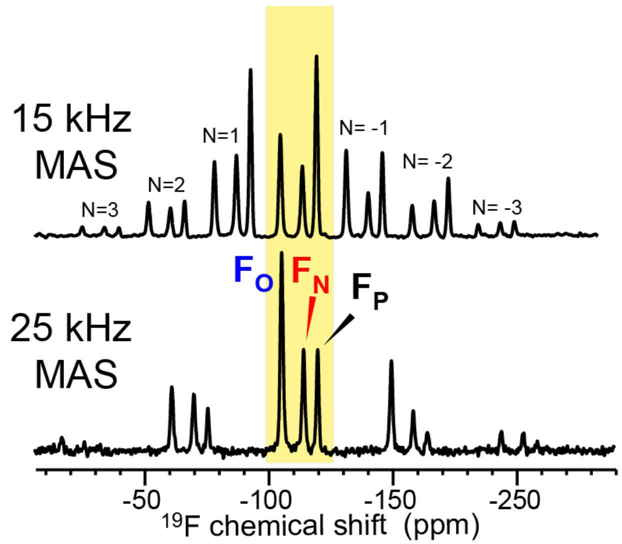

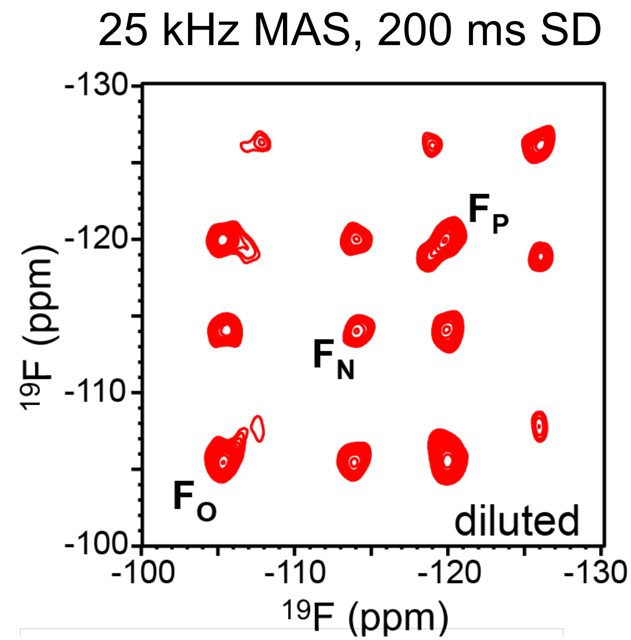

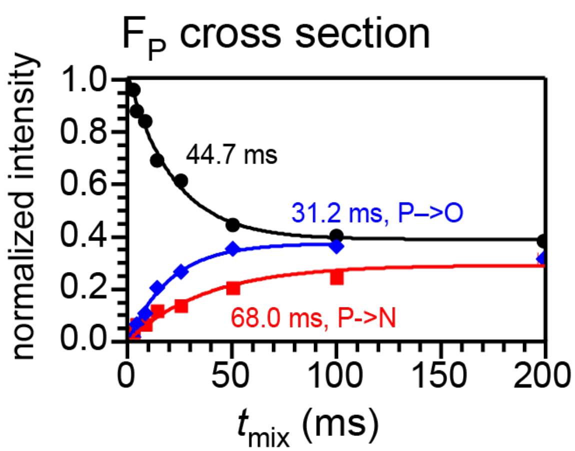

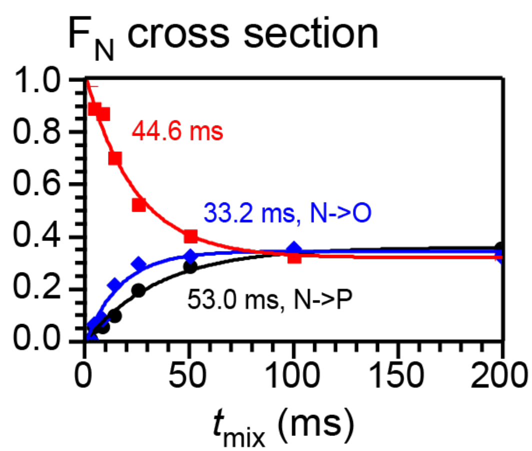

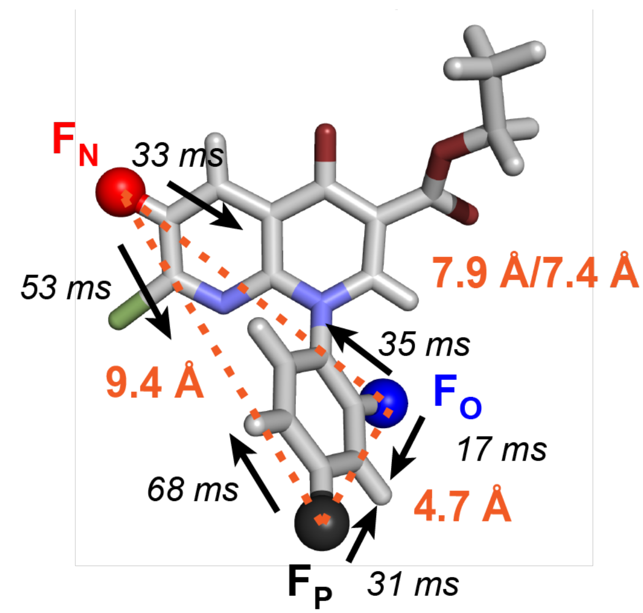

Distances: 4.7 – 9.4 Å

Buildup τ_{SD}: 17 – 68 ms

Roos, Wang, Shcherbakov, and Hong, ***J. Phys. Chem***, 122, 2900 (2018).

Spectrally Resolved ^{19}F Spin Exchange

25 kHz MAS

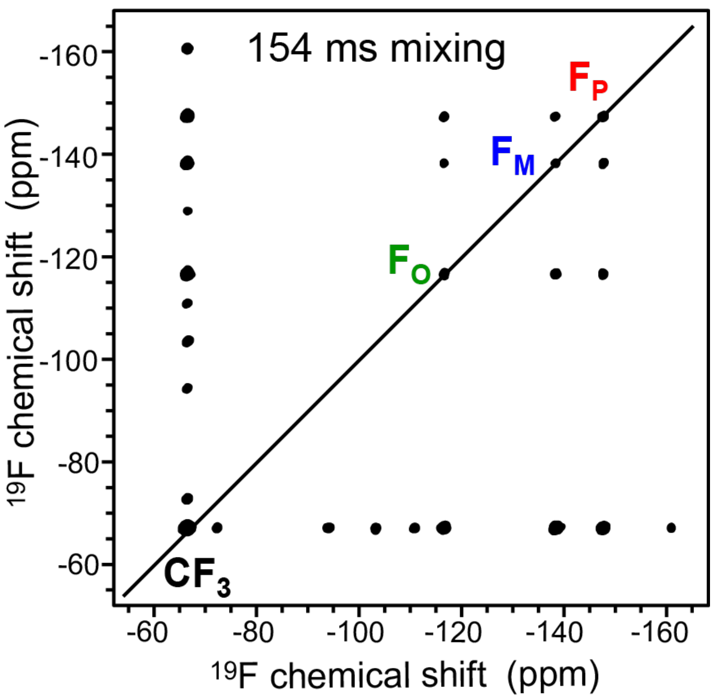

Sitagliptin

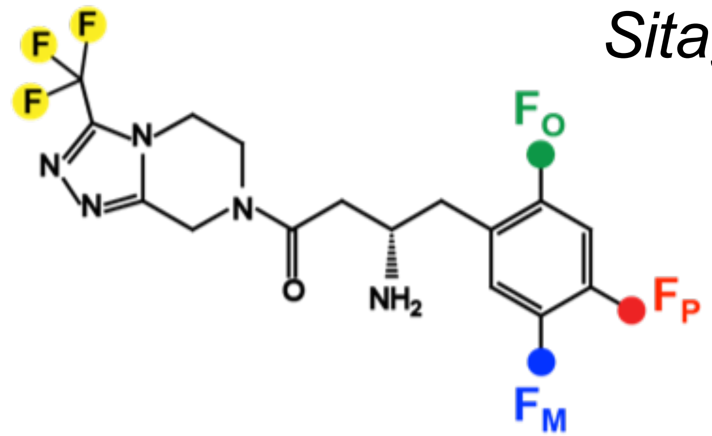

Distances: 2.7 – 9.6 Å

Buildup τ_{SD}: 6.7 – 40 ms

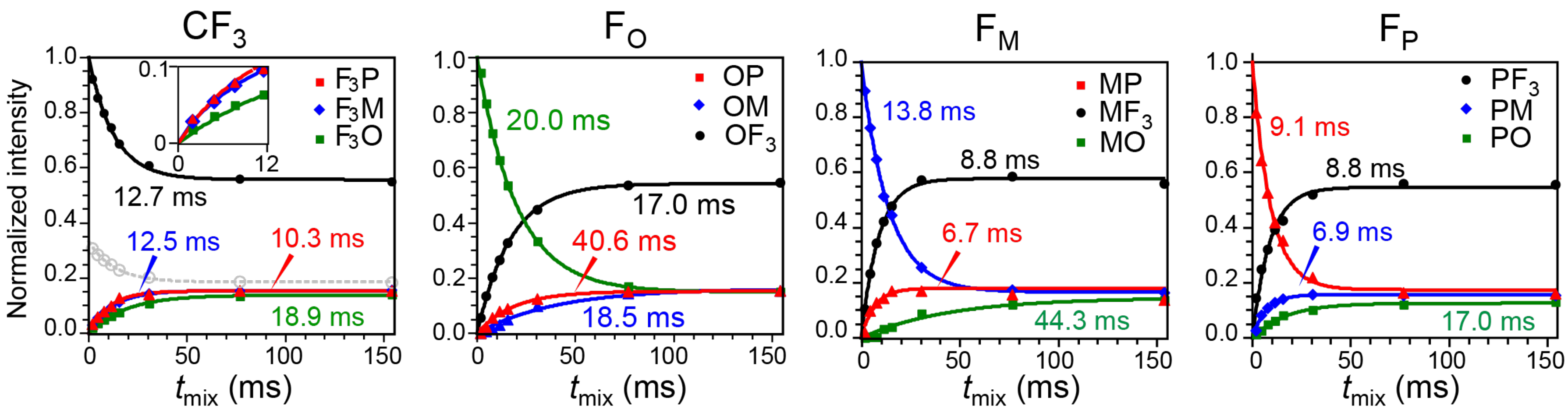

Roos, Wang, Shcherbakov, and Hong, ***J. Phys. Chem***, 122, 2900 (2018).

^{19}F-^{19}F Polarization Transfer in Proteins

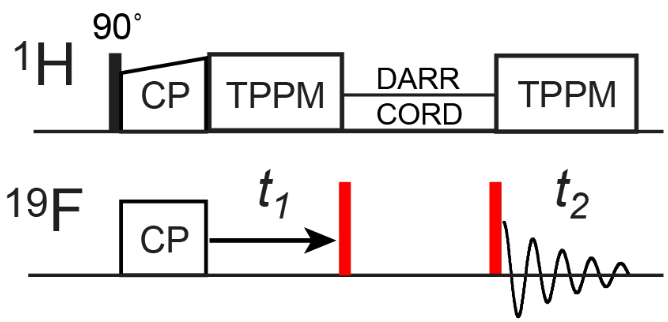

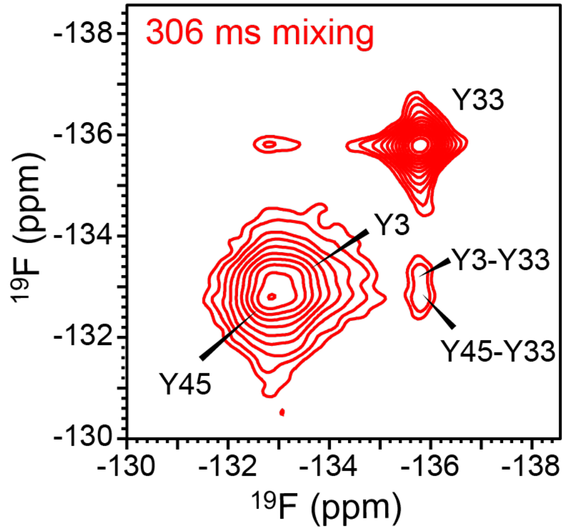

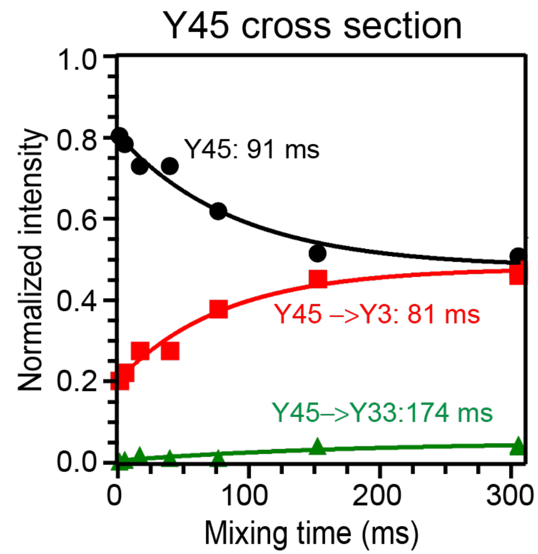

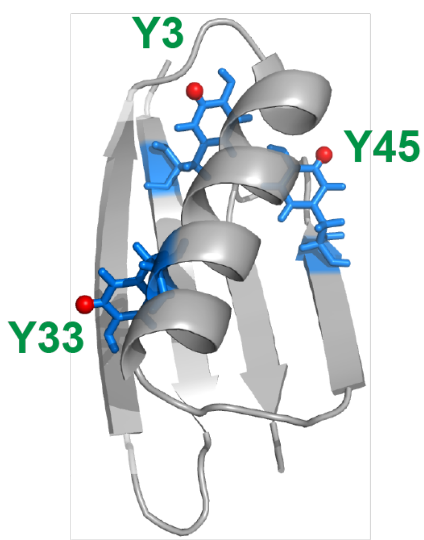

PDB: 2LGI

GB1

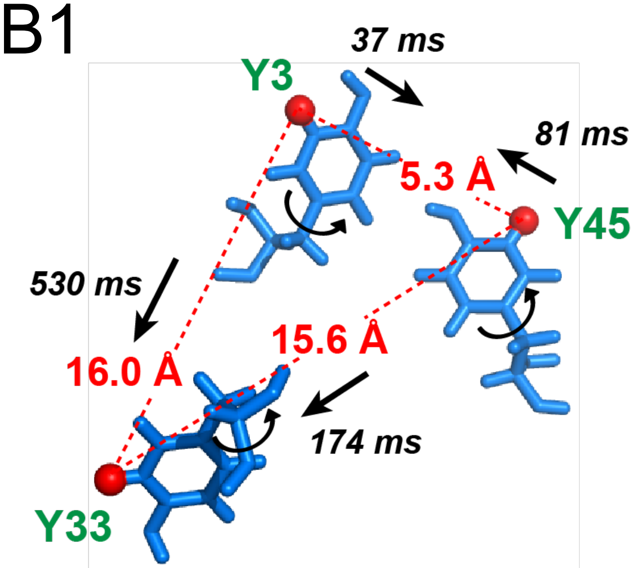

Roos, Wang, Shcherbakov, and Hong, ***J. Phys. Chem***, 122, 2900 (2018).

DARR/CORD is More Efficient Than PDSD

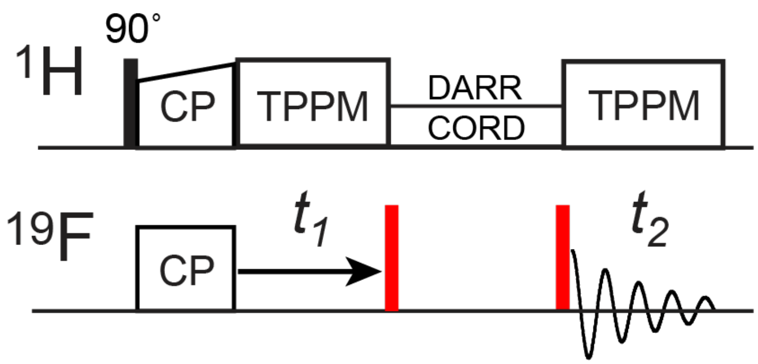

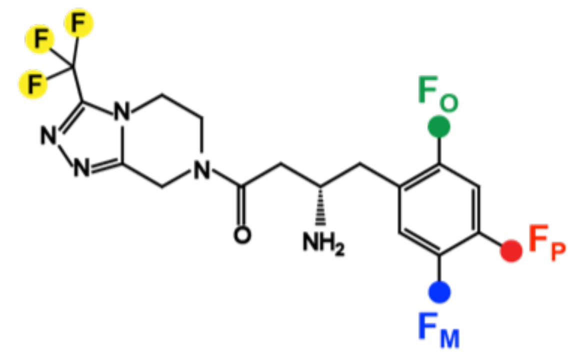

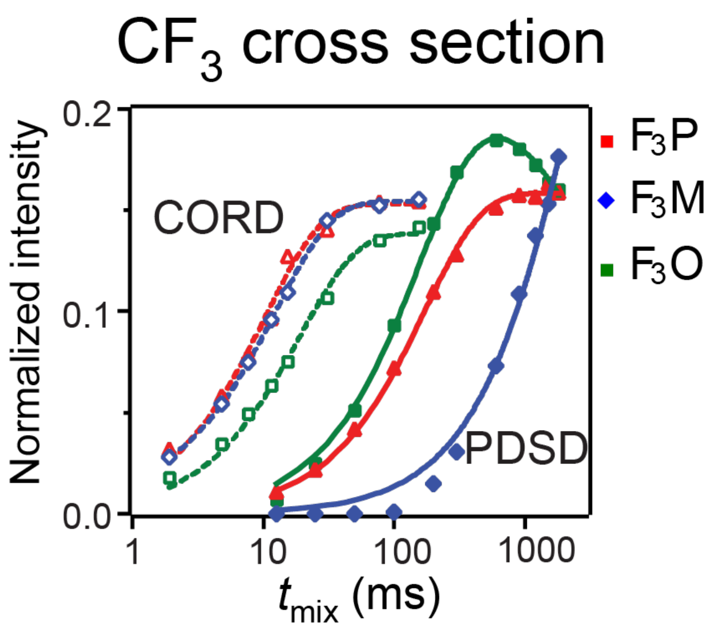

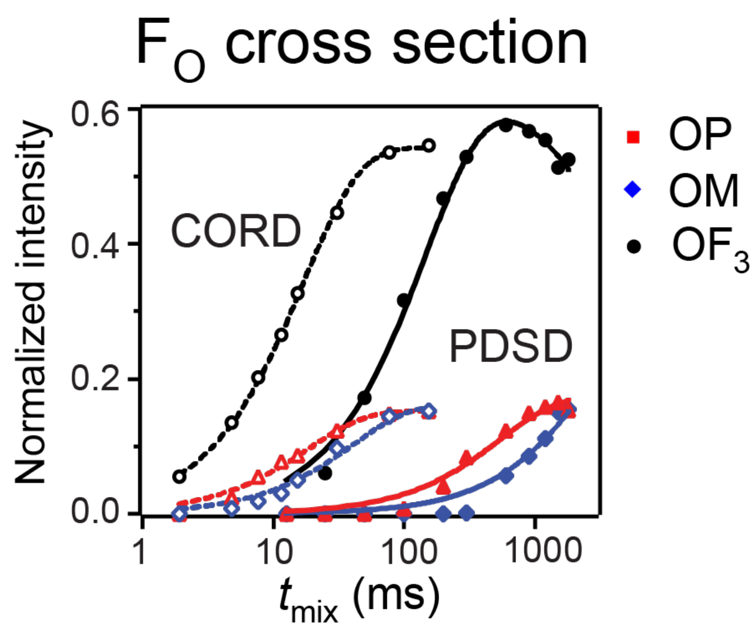

Roos, Wang, Shcherbakov, and Hong, ***J. Phys. Chem***, 122, 2900 (2018).

From Buildup Rates to Distances: Master Curves

$$k_{SD} \approx 0.5\pi F(0)\omega^2 \quad \text{where} \quad F(0) \approx f_0 / \Delta\delta_{\text{iso}}^2$$

$$\Rightarrow \quad k_{SD} \approx \frac{c}{\Delta\delta_{\text{iso}}^2} \frac{1}{r^6} \quad \Rightarrow \quad \log\left(k_{\text{SD}}\Delta\delta_{\text{iso}}^2\right) = \log c - 6\log r$$

Small CS differences, strong coupling limit

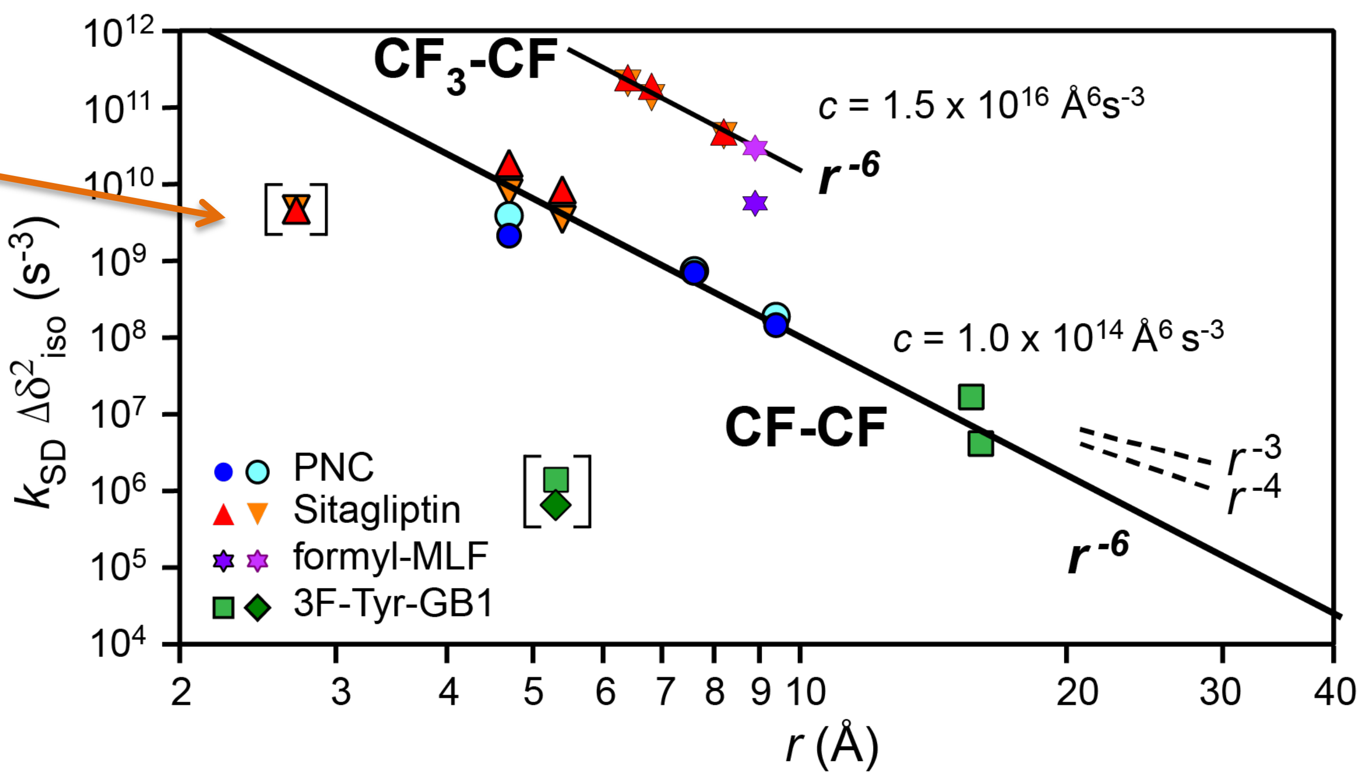

CF$_3$ groups: highly efficient polarization transfer.

Faster MAS: ^{19}F-^{19}F Dipolar Recoupling by RFDR

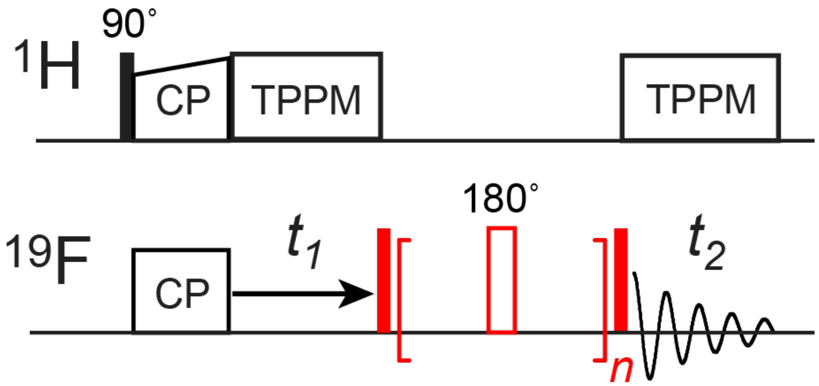

1 nm : ~5 ms to reach equilibrium

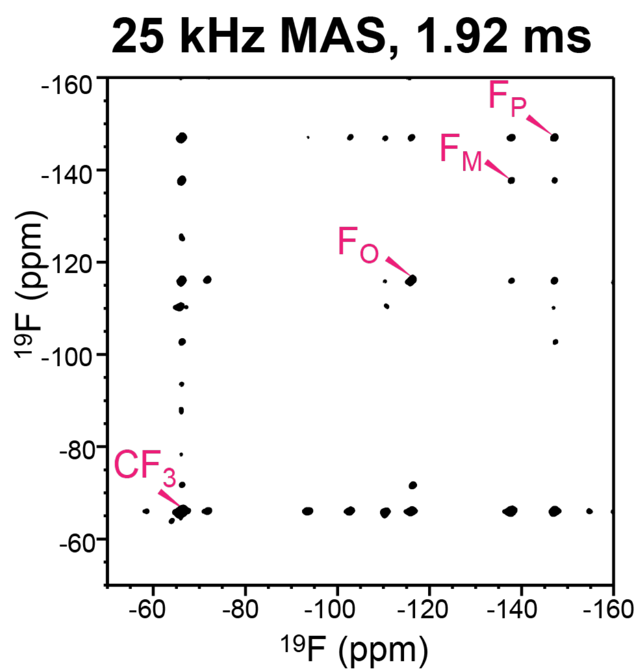

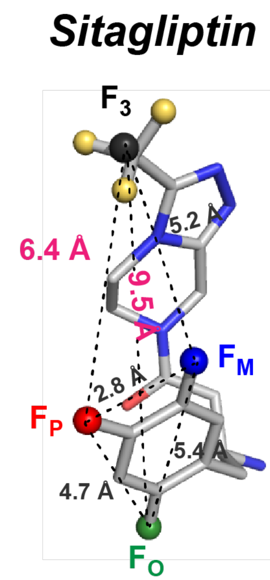

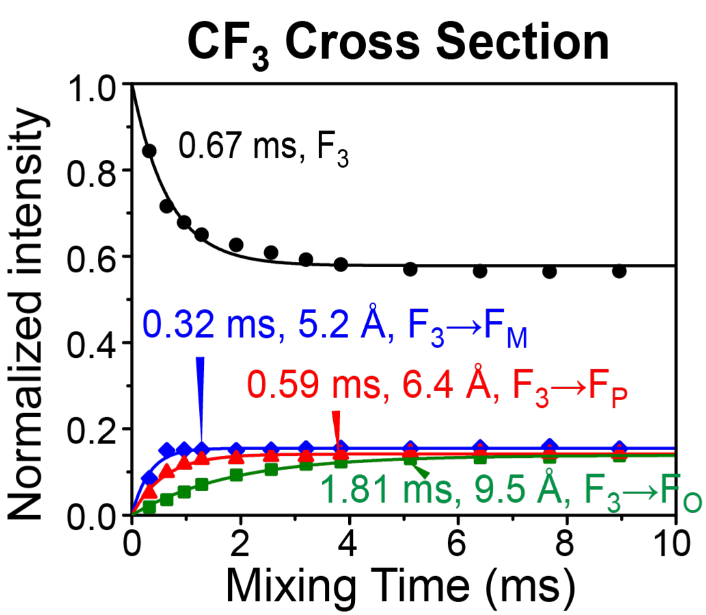

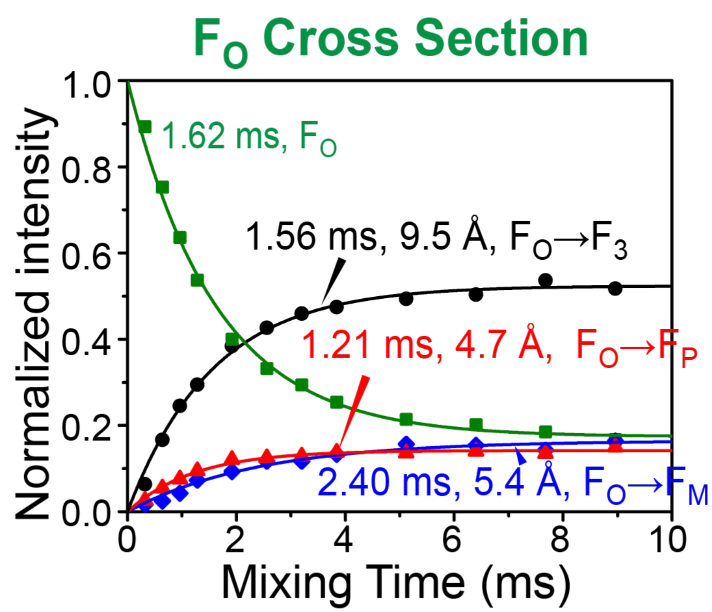

^{19}F RFDR: formyl-MLF

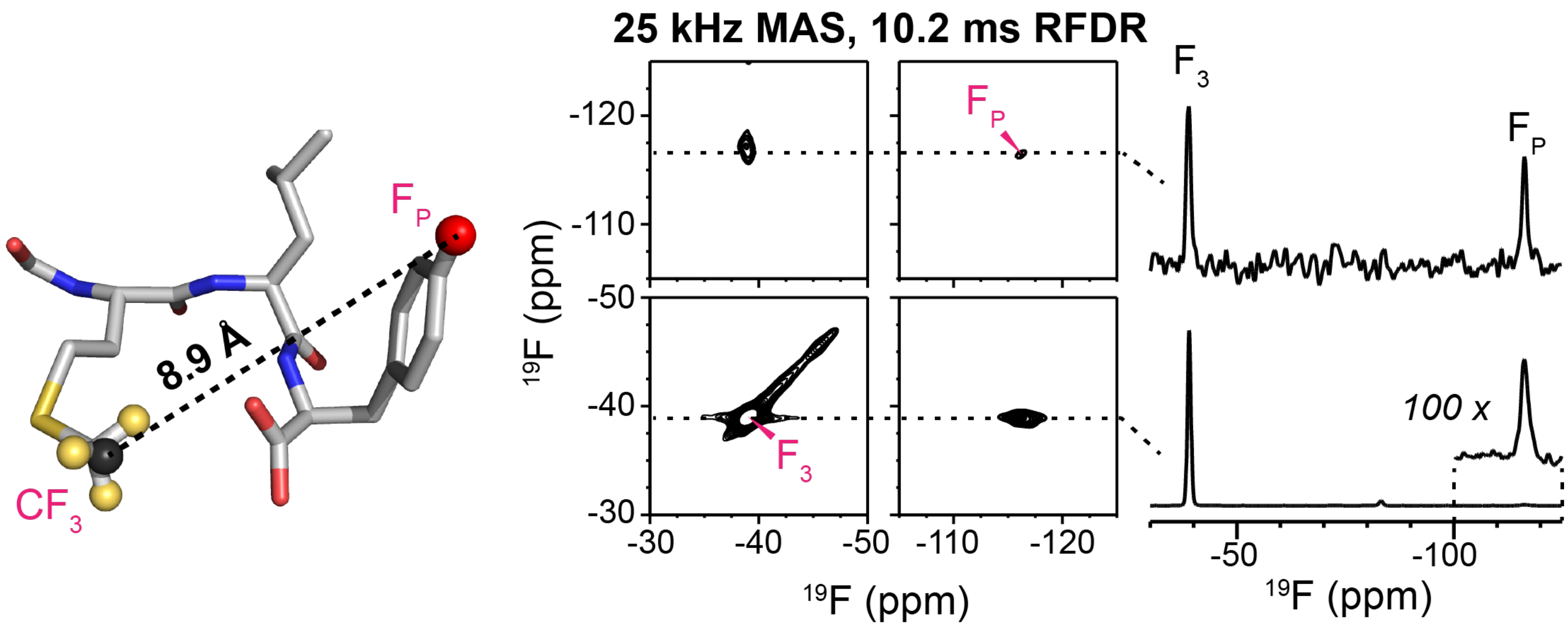

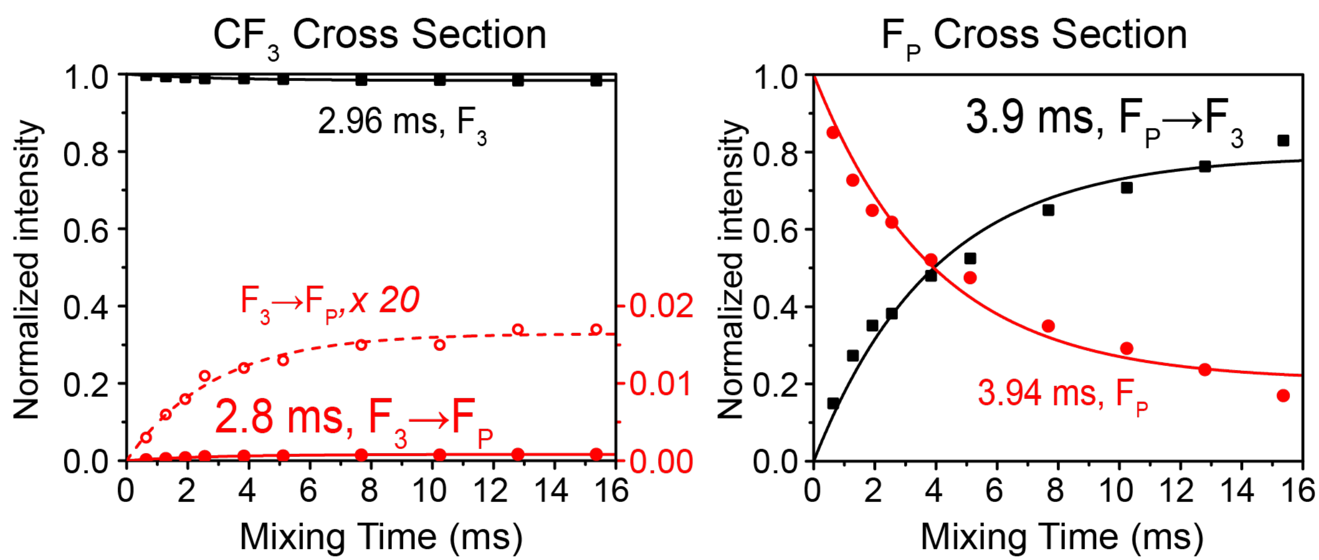

Roos, Mandala and Hong, ***J. Phys. Chem.***, 122, 9302 (2018).

^{19}F RFDR is More Efficient at Faster MAS

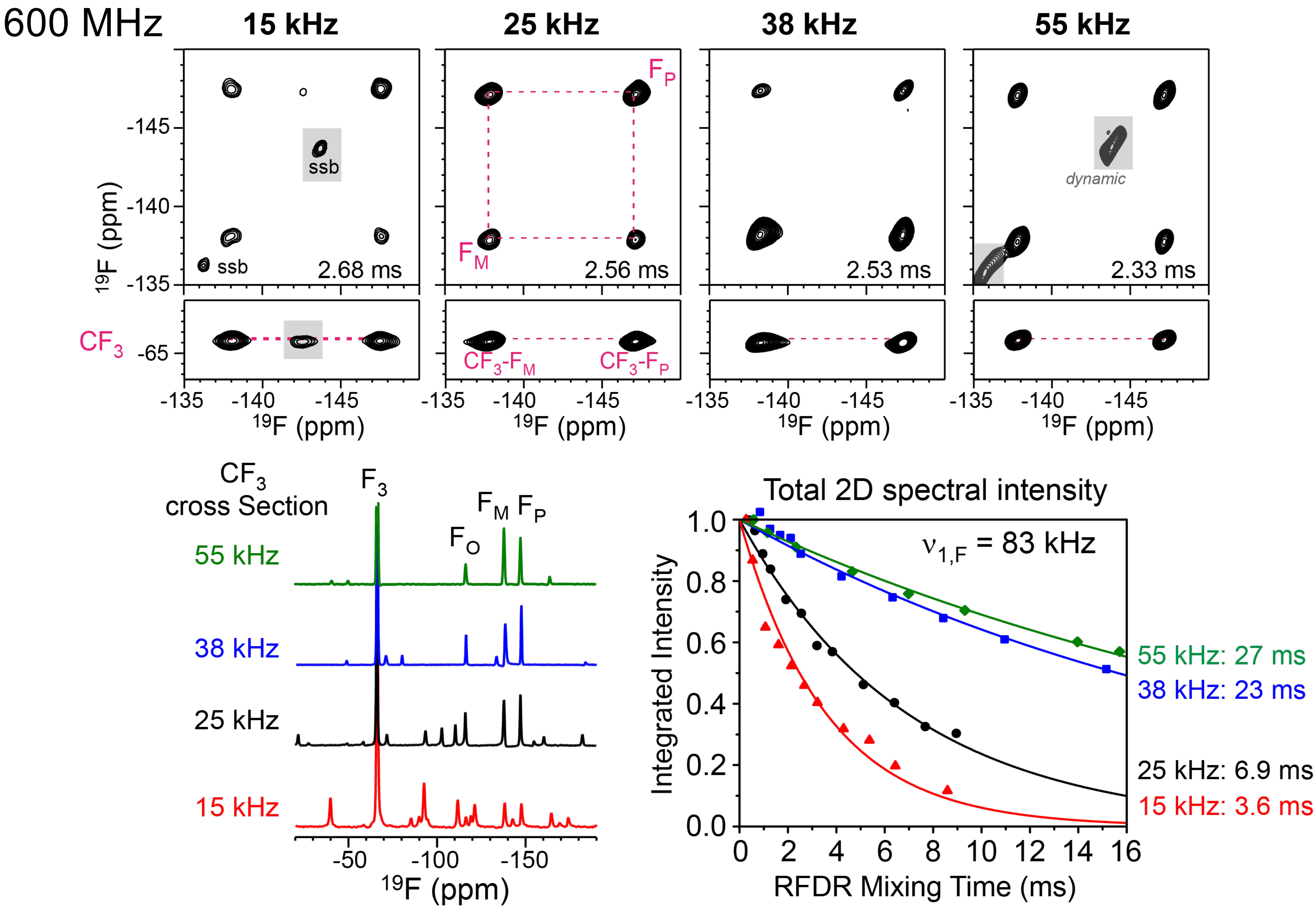

Roos, Mandala and Hong, ***J. Phys. Chem.***, 122, 9302 (2018).

^{19}F CSA Tensor Orientation & Relayed Transfer

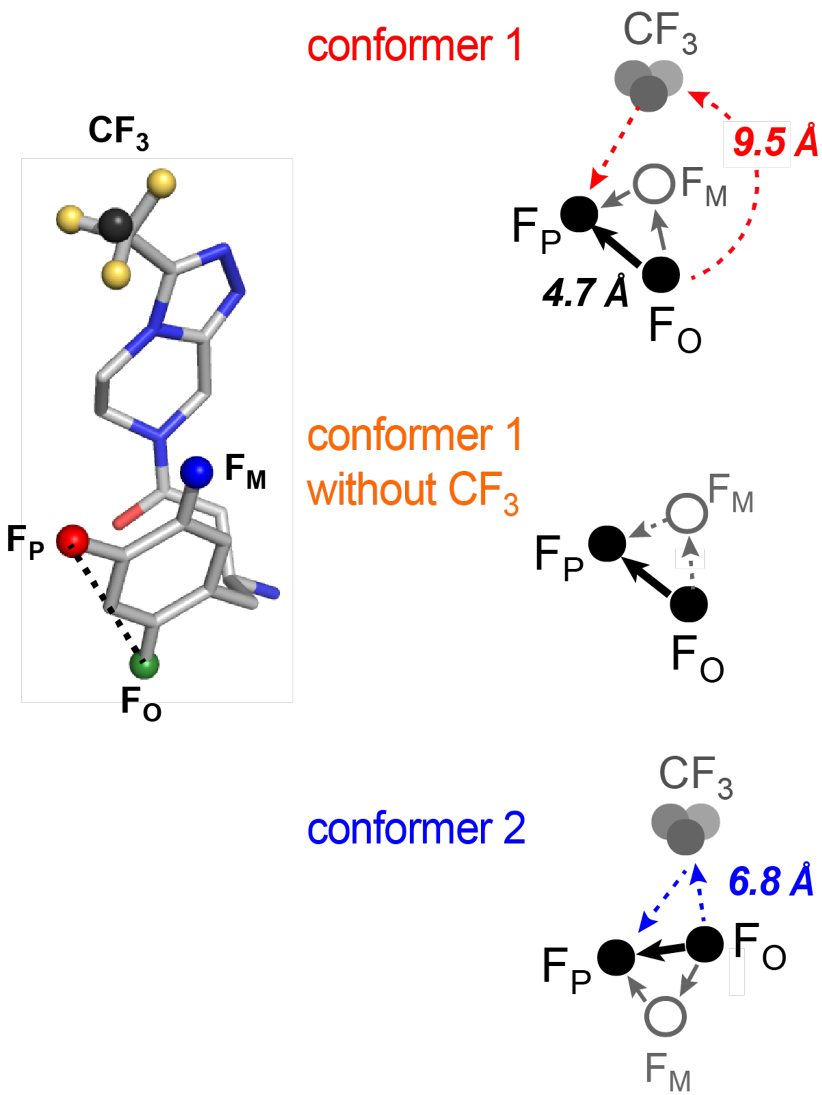

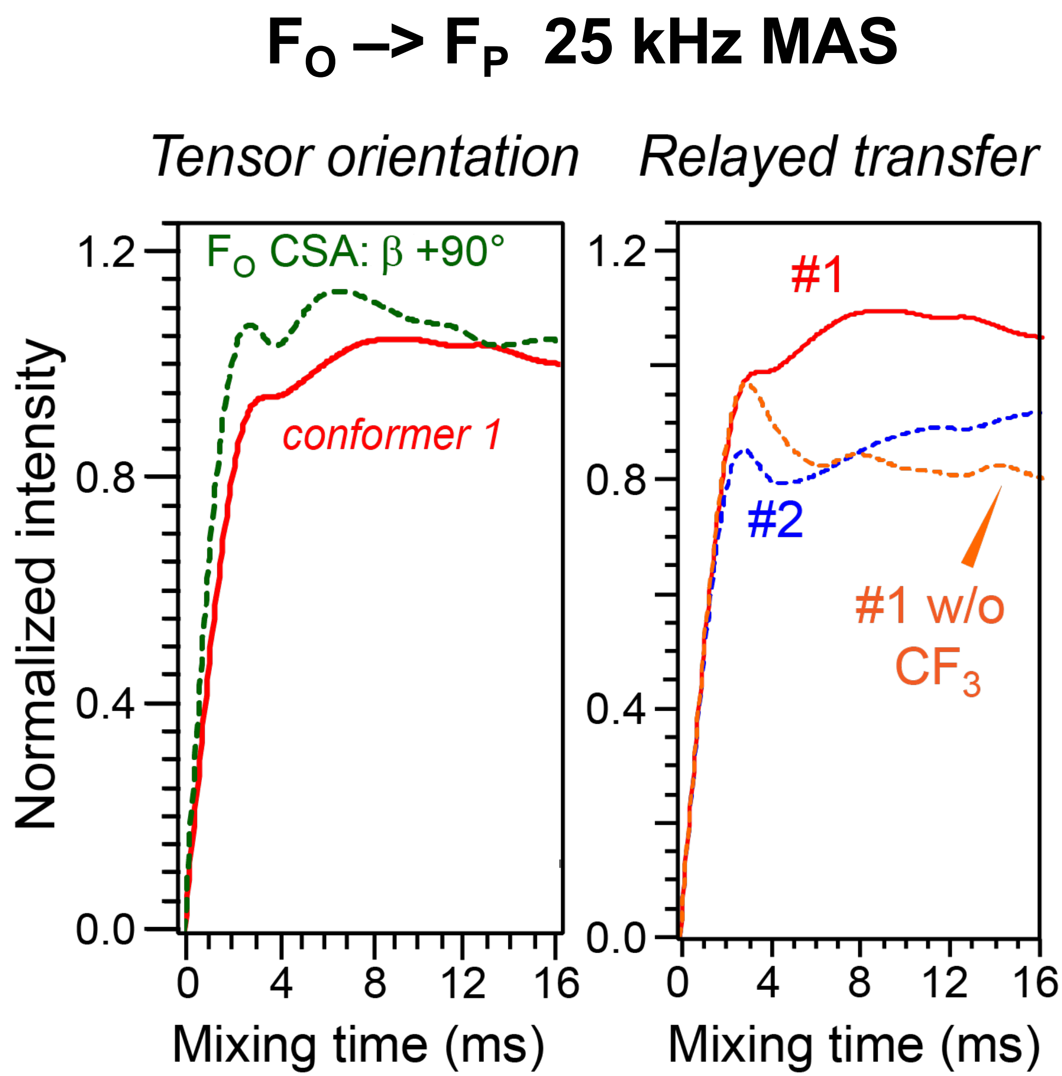

Roos, Mandala and Hong, ***J. Phys. Chem.***, 122, 9302 (2018).

Finite Pulse Lengths & CSA Orientation

δ-pulse regime | **intermediate regime** | **finite-pulse regime**

ν_r = 25 kHz, ^{19}F ν_1 = 83 kHz | ν_r = 38 kHz, ^{19}F ν_1 = 63 kHz | ν_r = 60 kHz, ^{19}F ν_1 = 50 kHz

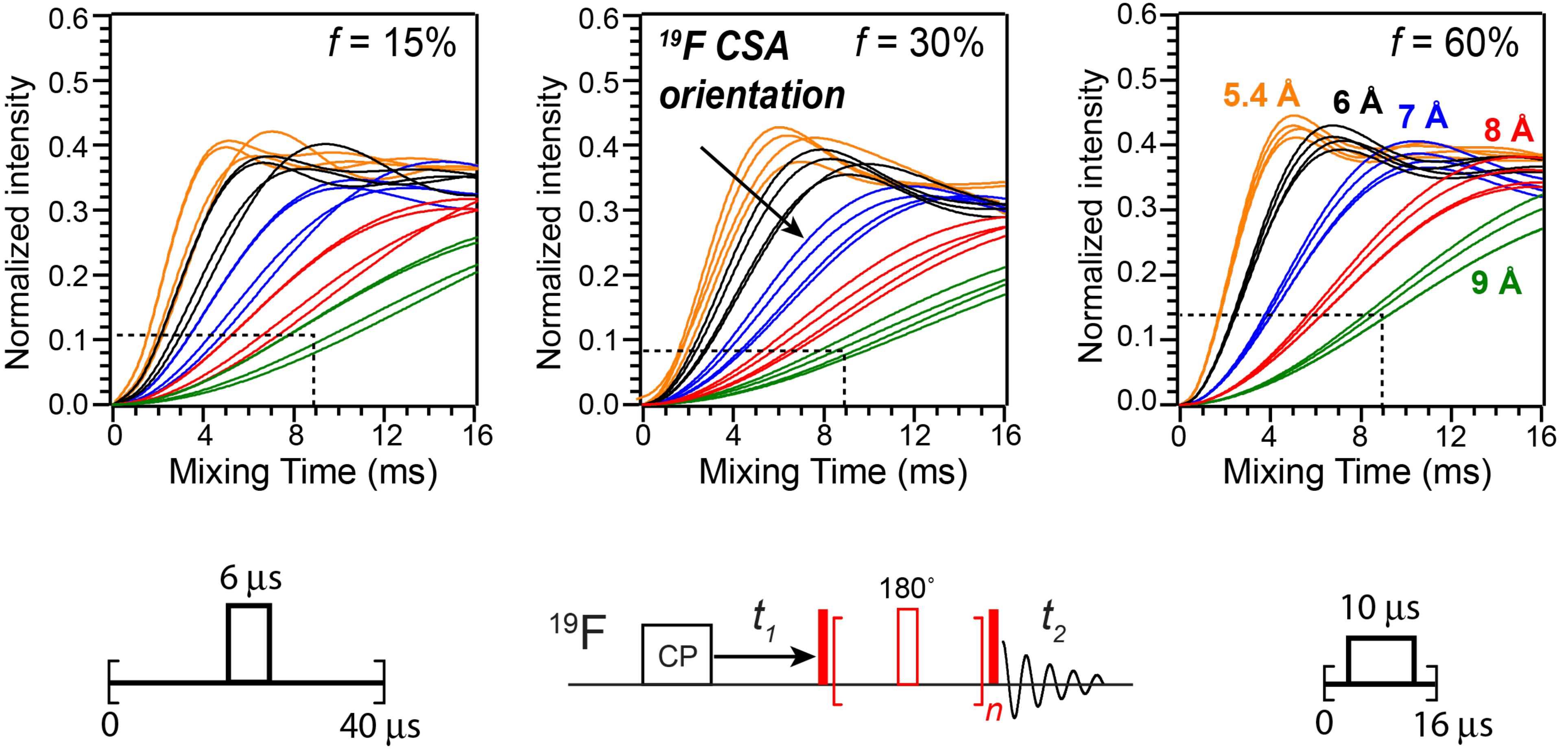

HONG LAB

Finite-Pulse RFDR at Fast MAS is More Efficient Than δ-Pulse RFDR at Slow MAS

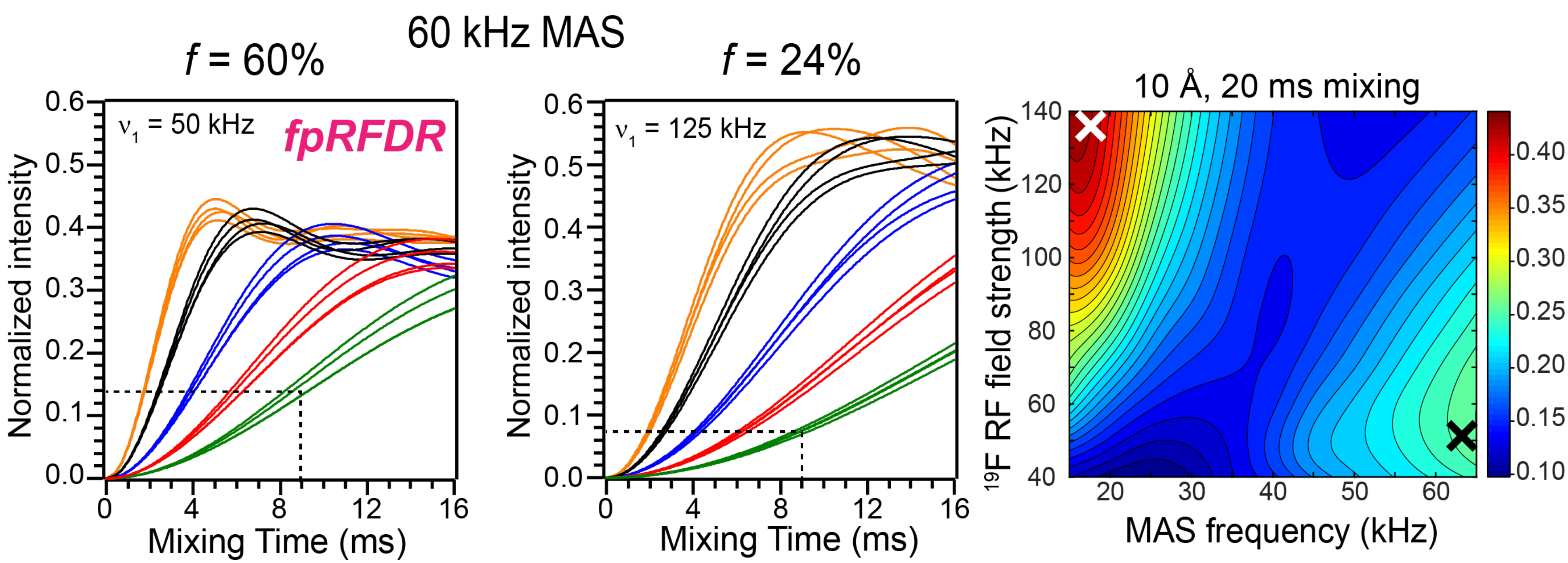

Roos, Mandala and Hong, ***J. Phys. Chem.***, 122, 9302 (2018).

Homonuclear 2D ^{19}F-^{19}F Spin Exchange for Chemically Equivalent Spins (Anisotropic Spin Exchange)

Anisotropic ^{19}F Spin Exchange: CODEX

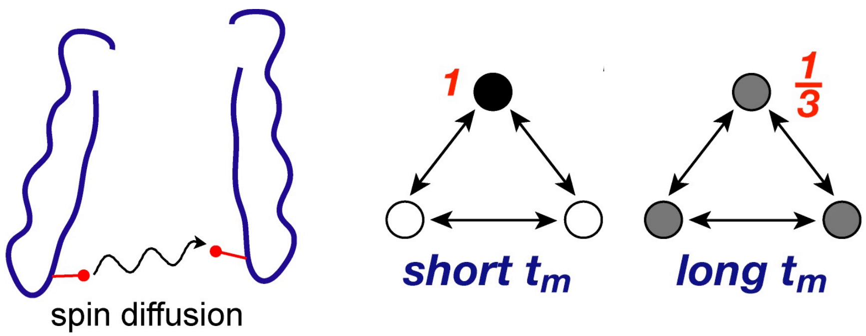

deAzevedo… Schmidt-Rohr, ***J. Am. Chem. Soc***, 121, 8411 (1999).

- Equilibrium echo intensity is 1/N for an oligomeric number of N;

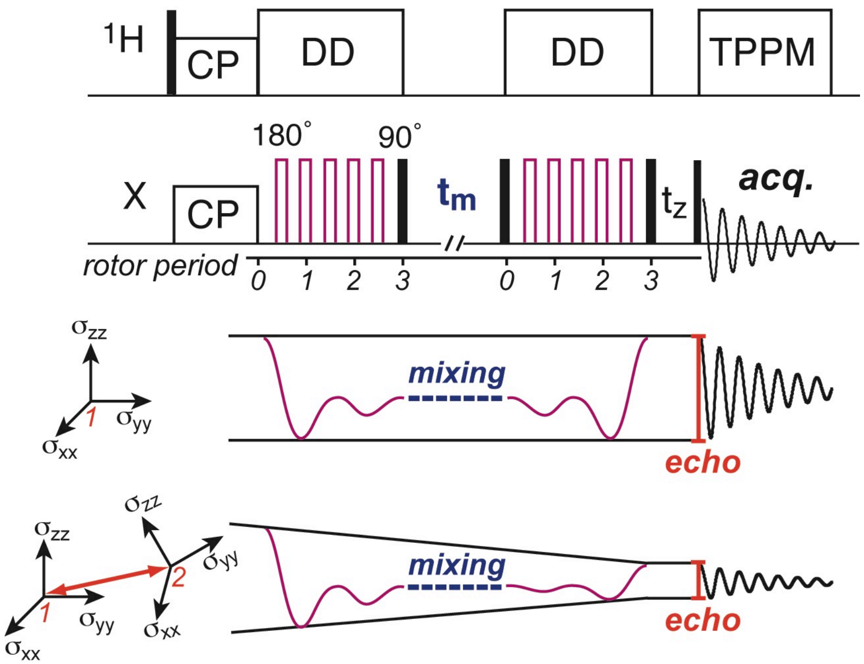

$$\overrightarrow{M(t)} = e^{-Kt}\,\overrightarrow{M(0)}$$

$$K = \begin{pmatrix} k_{AB} + k_{AC} & -k_{BA} & -k_{CA} \\ -k_{AB} & k_{BA} + k_{BC} & -k_{CB} \\ -k_{AC} & -k_{BC} & k_{CA} + k_{CB} \end{pmatrix}$$

$$k_{ij} = 0.5\pi\,\omega_{ij}^2\,F(0)$$

Luo and Hong, ***J. Am. Chem. Soc.*** 128, 7242 (2006).

^{19}F CODEX of SARS ETM in Lipid Bilayers

ERGIC membrane: POPC, POPE, POPS, PI, Chol

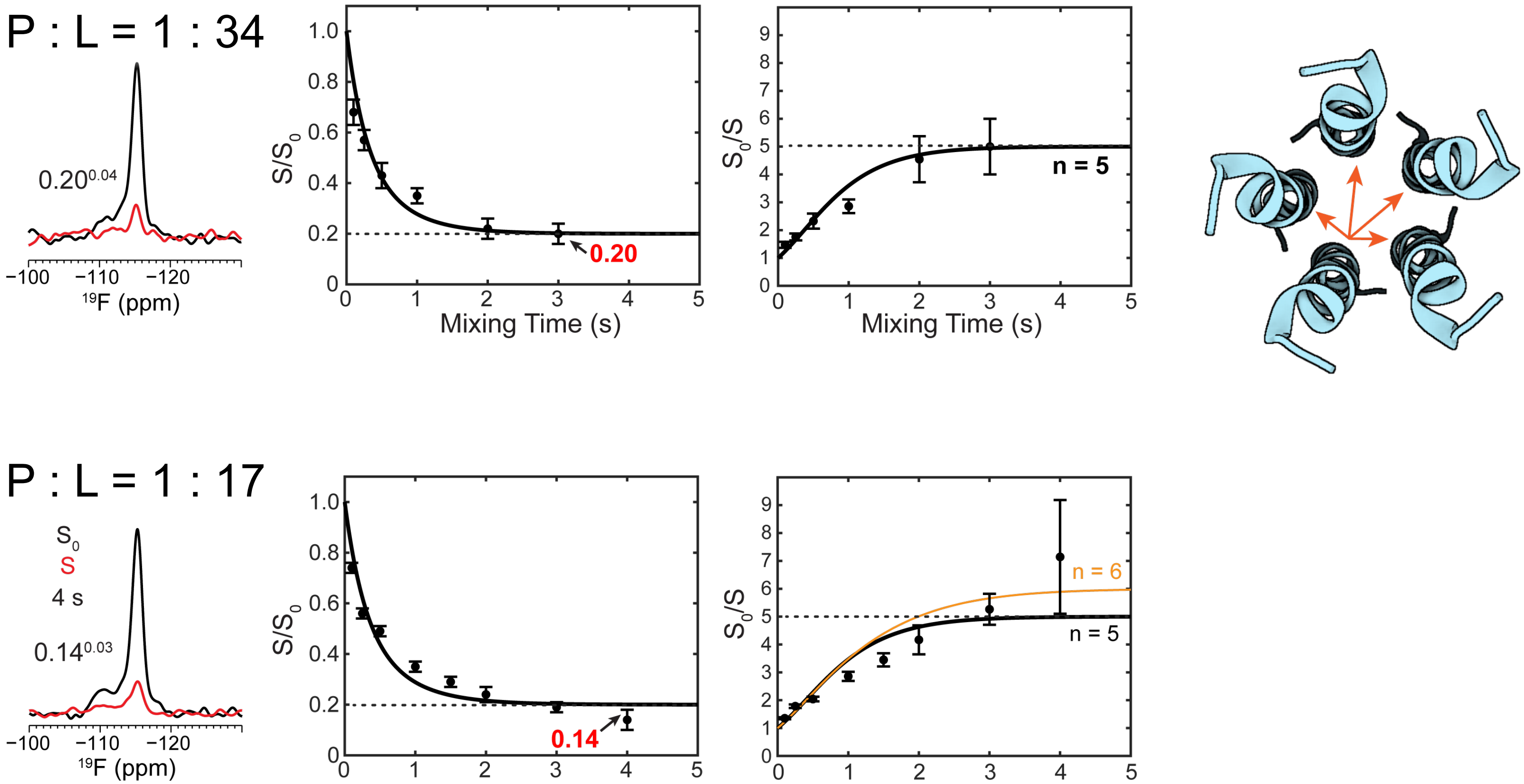

^{19}F CODEX at 15 – 35 kHz MAS

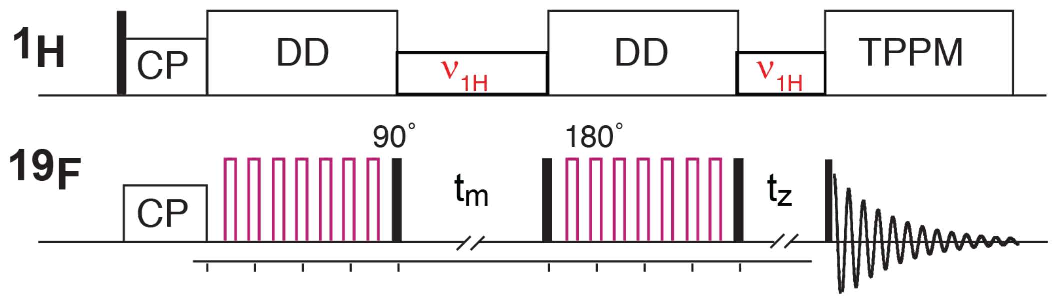

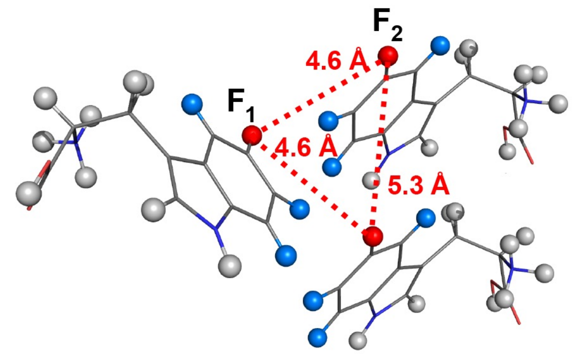

^{1}H decoupling field dependence 25 kHz MAS

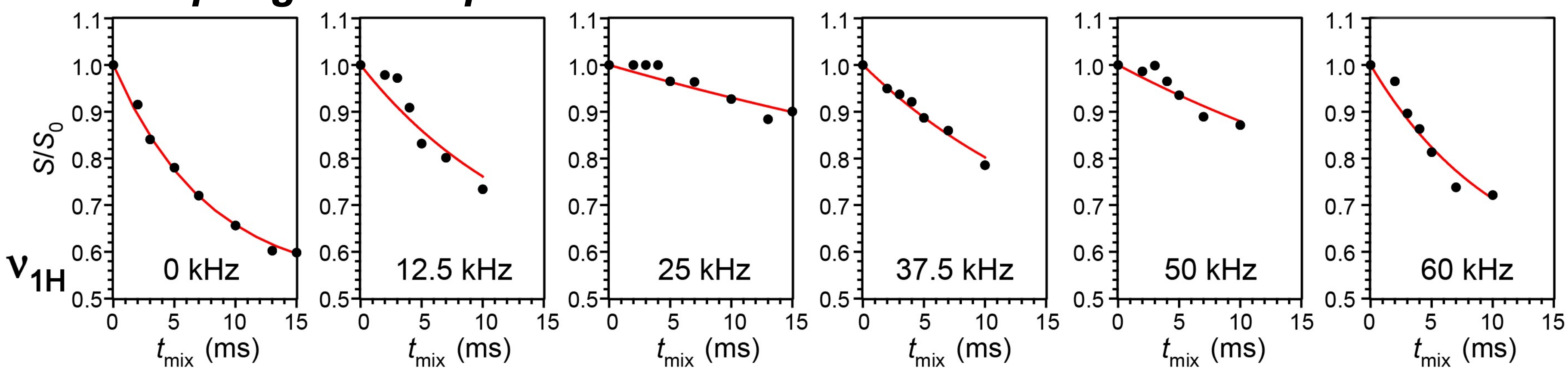

MAS dependence

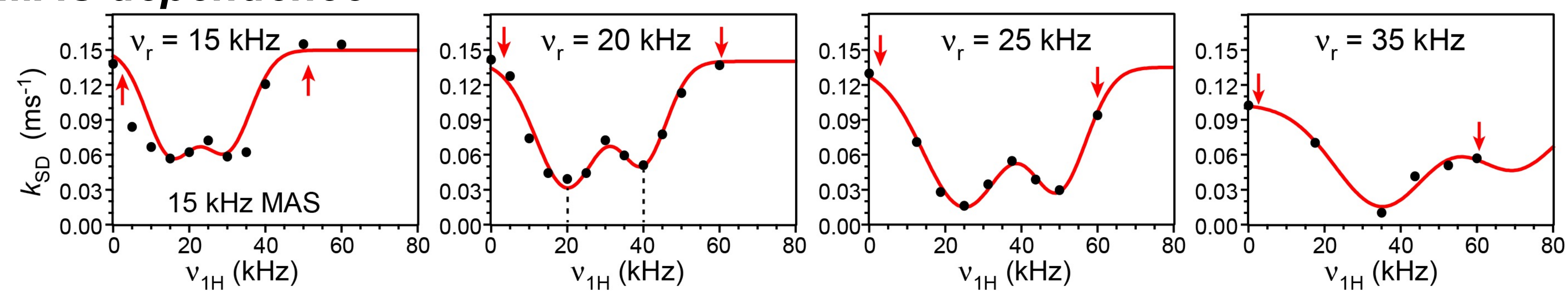

Roos, Wang, Shcherbakov, and Hong, ***J. Phys. Chem***, 122, 2900 (2018).

Bruker HFX Probe

- One RF input for ^{1}H & ^{19}F channels;
- Isolation between ^{1}H and ^{19}F channels achieved by connecting tuning components at different locations on the $\lambda/4$ transmission line.

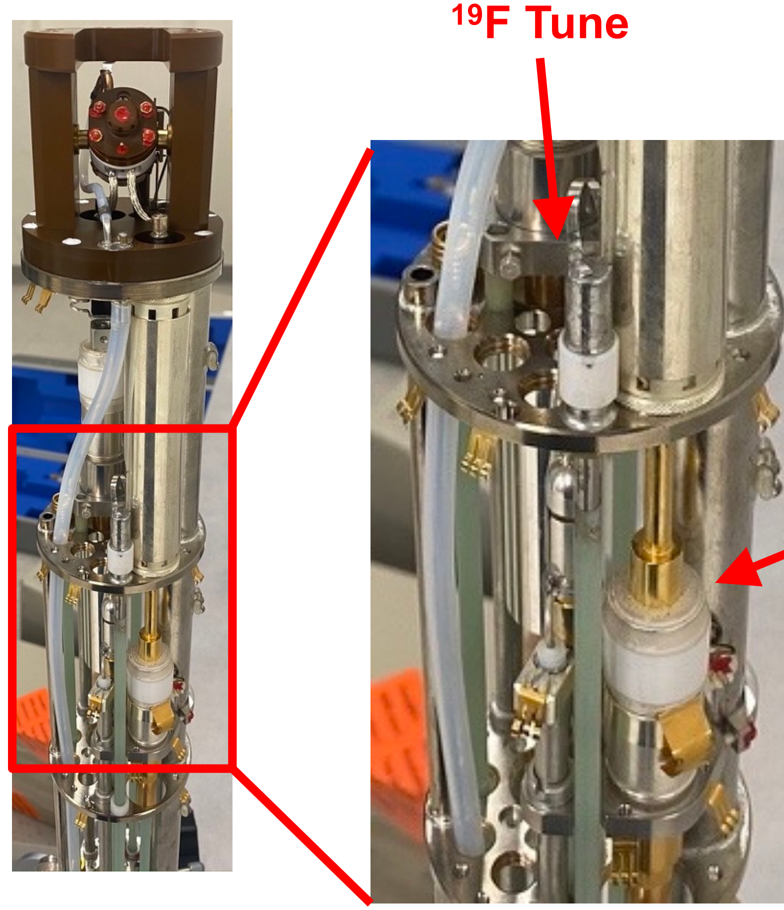

Bruker HFX Probe Design

Circuitry with detailed components for $\lambda/2$ line:

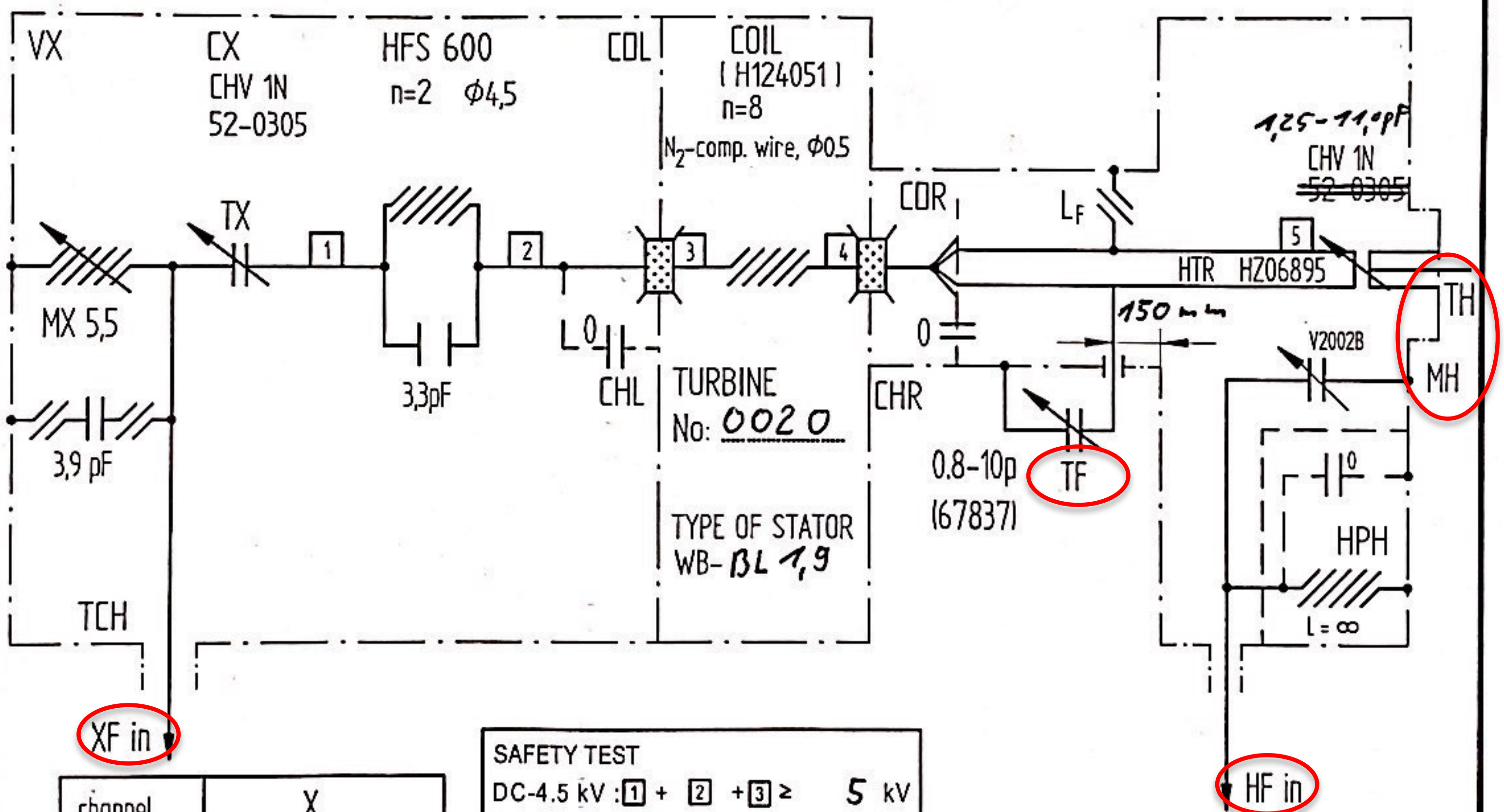

channel	X	
f_U / MHz	179,5	
f_L / MHz	49,6	
nucleus	15N	13C
Q_m	65	105

SAFETY TEST
DC-4.5 kV : [1] + [2] + [3] ≥ 5 kV
DC-4.5 kV : [4] + HTR + [5] ≥ 5 kV

nucleus	^{19}F	^{1}H
Transmission line	$\lambda/4$	
Q_m	180	240
Δf_s / MHz	4,64	8,8

Converting a 1.3 mm HCN Probe to an FCN Probe

Adjustable λ/4 transmission line screw position allows easy switch between ^{1}H and ^{19}F tuning frequencies.

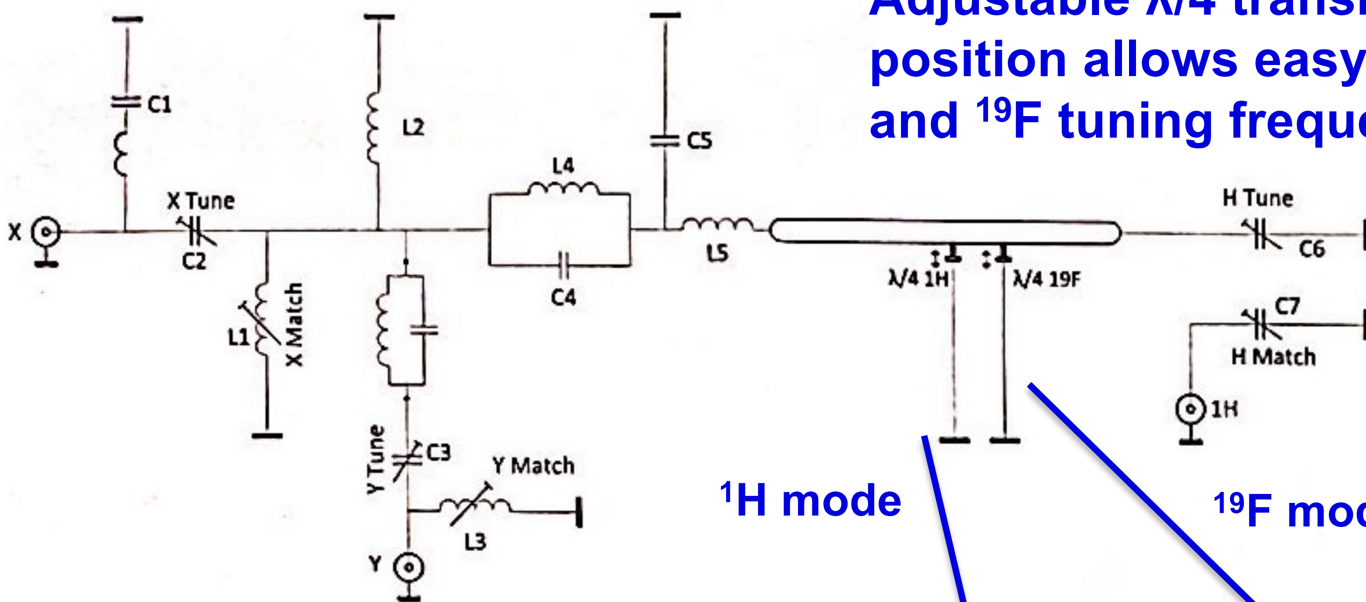

^{1}H mode

^{19}F mode

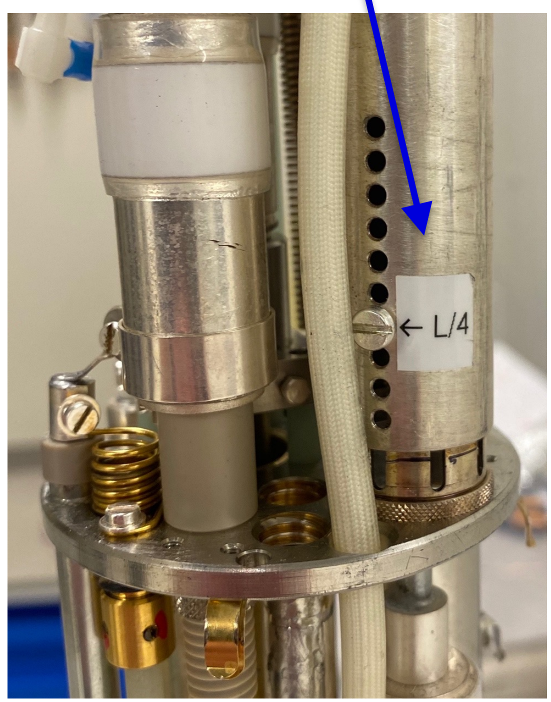

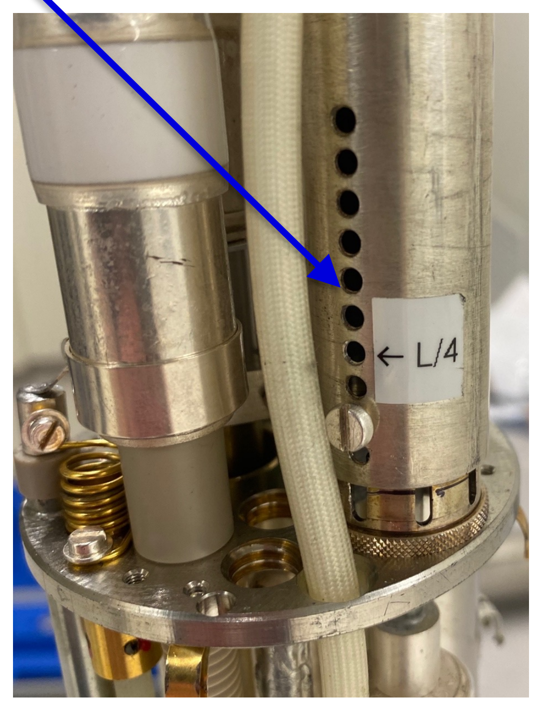

Part 2

Heteronuclear X-^{19}F Distance Experiments by REDOR

Rotational Echo Double Resonance (REDOR)

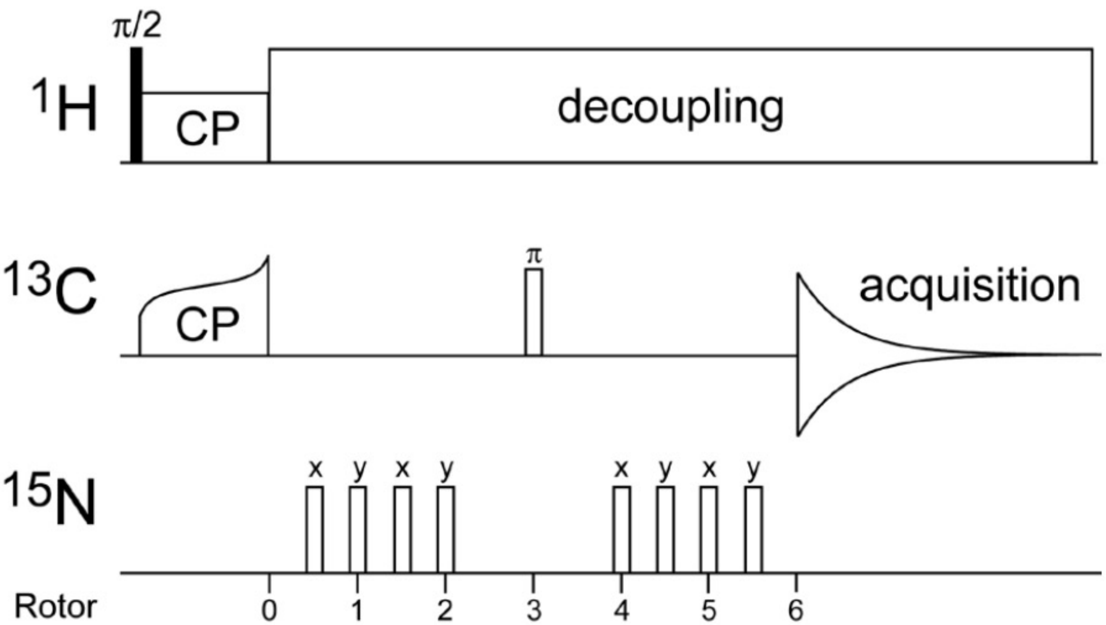

- Rotor synchronized spin-echo on ^{13}C channel refocuses ^{13}C isotropic chemical shift and CSA evolution
- Recoupled ^{15}N CSA commutes with ^{13}C-^{15}N DD coupling!
- 2nd group of pulses shifted by $-\tau_r/2$ relative to 1st group to change sign of H_D and avoid refocusing the ^{13}C-^{15}N dipolar coupling
- *xy*-type phase cycling of ^{15}N pulses is critical (**Gullion, JMR 1990**)

REDOR Universal Curve: Example

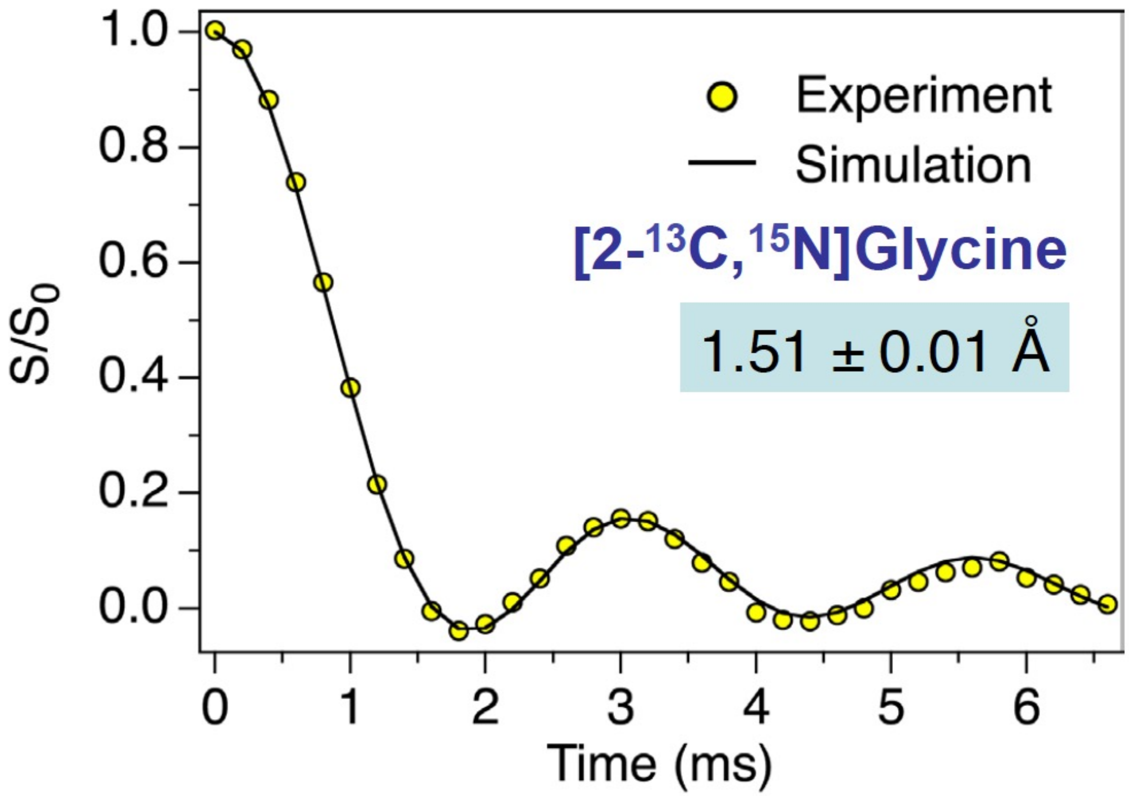

- Experiment highly robust toward ^{15}N CSA, experimental imperfections, resonance offset and finite pulse effects (**xy-4/xy-8 phase cycling is critical for this**)
- REDOR is used routinely to measure distances up to ~5-6 Å (D ~ 20 Hz) in isolated ^{13}C-^{15}N spin pairs

2D ^{13}C-^{19}F and ^{1}H-^{19}F REDOR Experiments

1D ^{13}C-^{19}F REDOR

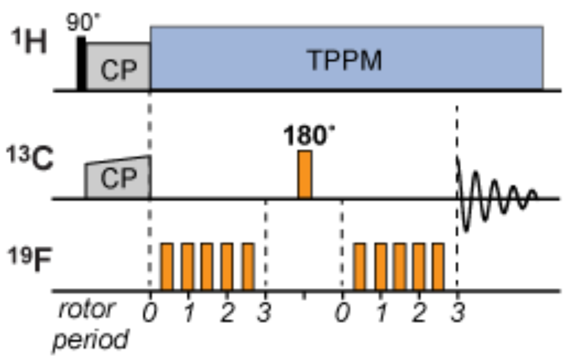

2D CC Resolved ^{13}C-^{19}F REDOR

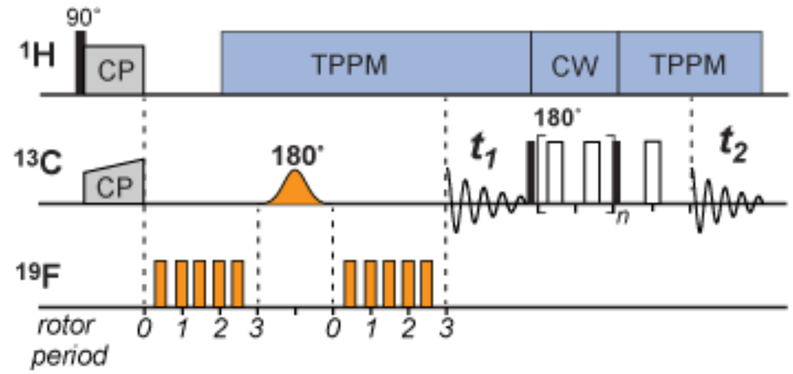

Shcherbakov et al, ***JPC***, 2018

2D hNH Resolved ^{1}H-^{19}F REDOR

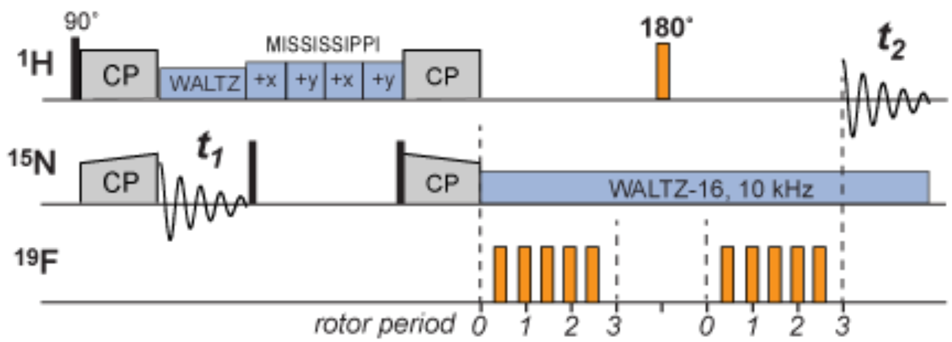

Shcherbakov et al, ***JPC***, 2019

2D CC Resolved ^{1}H-^{19}F REDOR

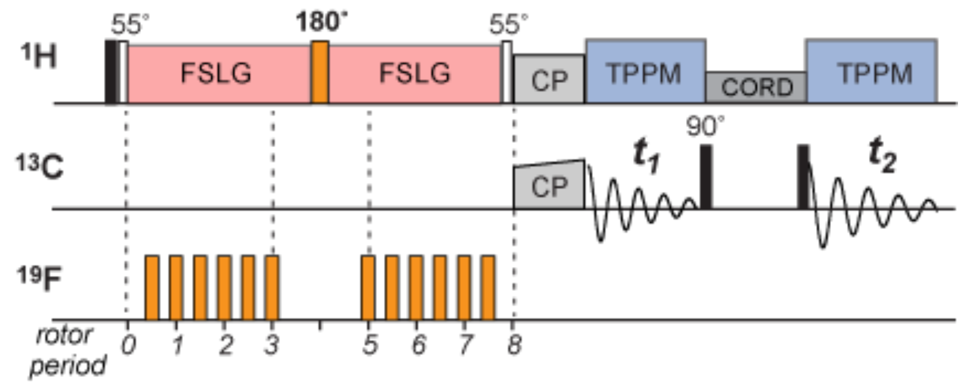

Duan et al, ***JACS***, 2022

Multiplexing: 2D-Resolved ^{13}C-^{19}F Distances

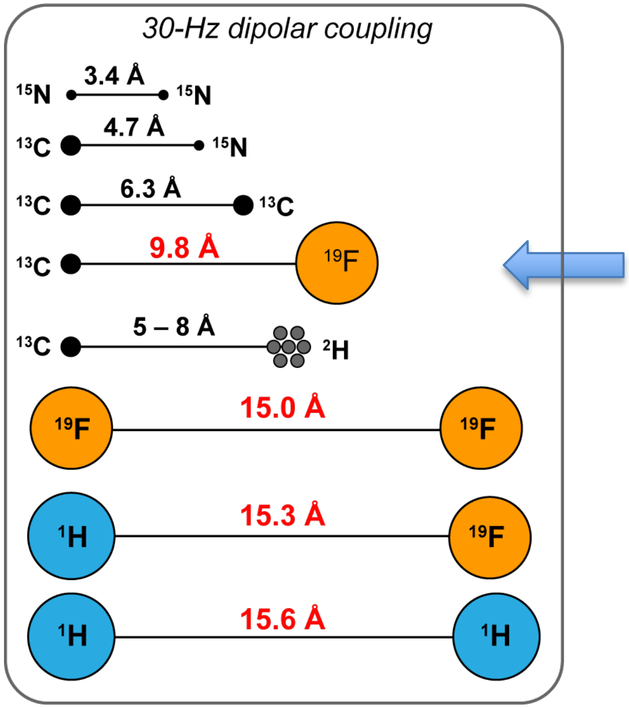

2D CC Resolved ^{13}C-^{19}F REDOR

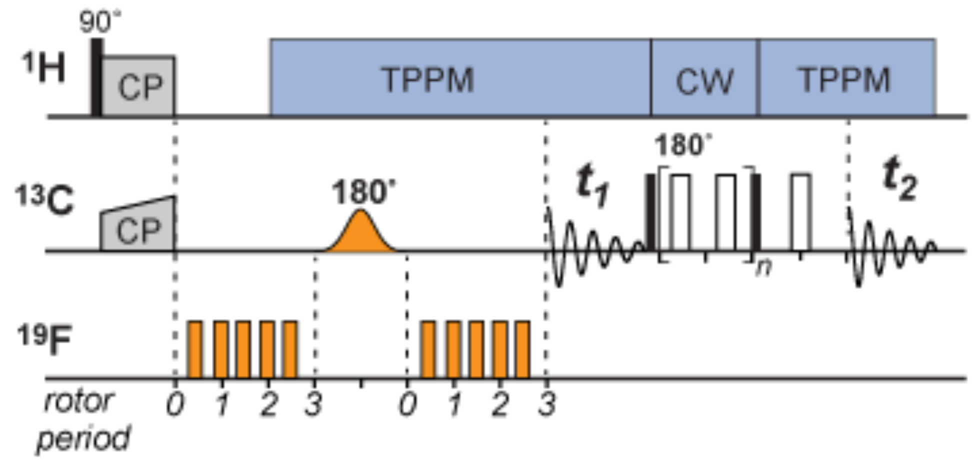

^{19}F CSA Dependence

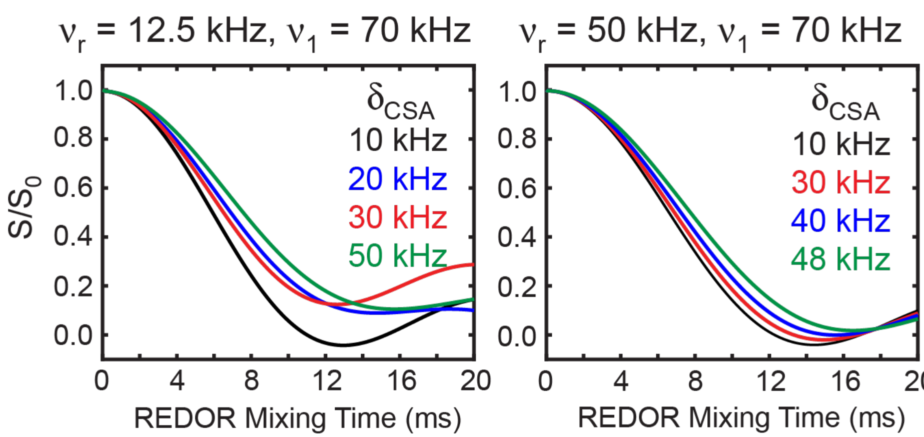

MAS Dependence

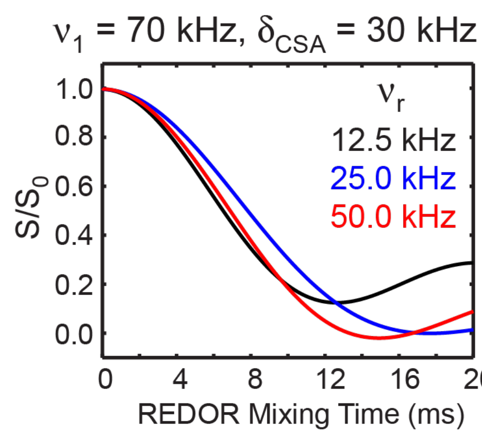

Distance curves

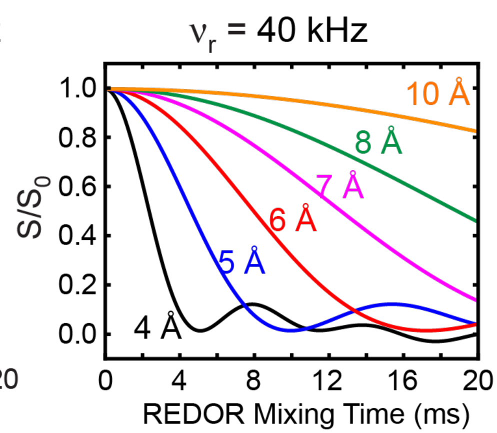

Fast MAS (40-50 kHz) retrieves near-universal REDOR dephasing.

2D-Resolved ^{13}C-^{19}F REDOR Spectra

600 MHz, 25 kHz MAS, 8.4 ms mixing

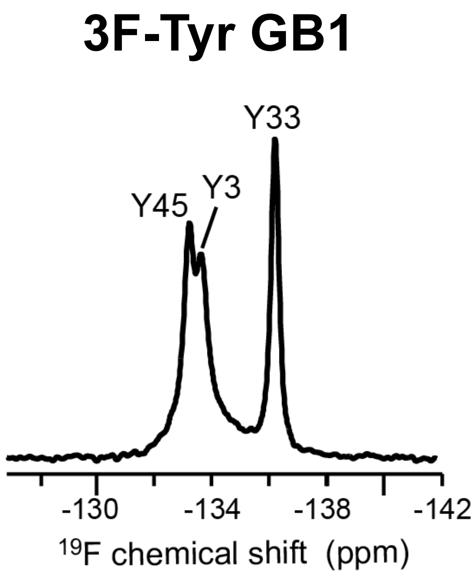

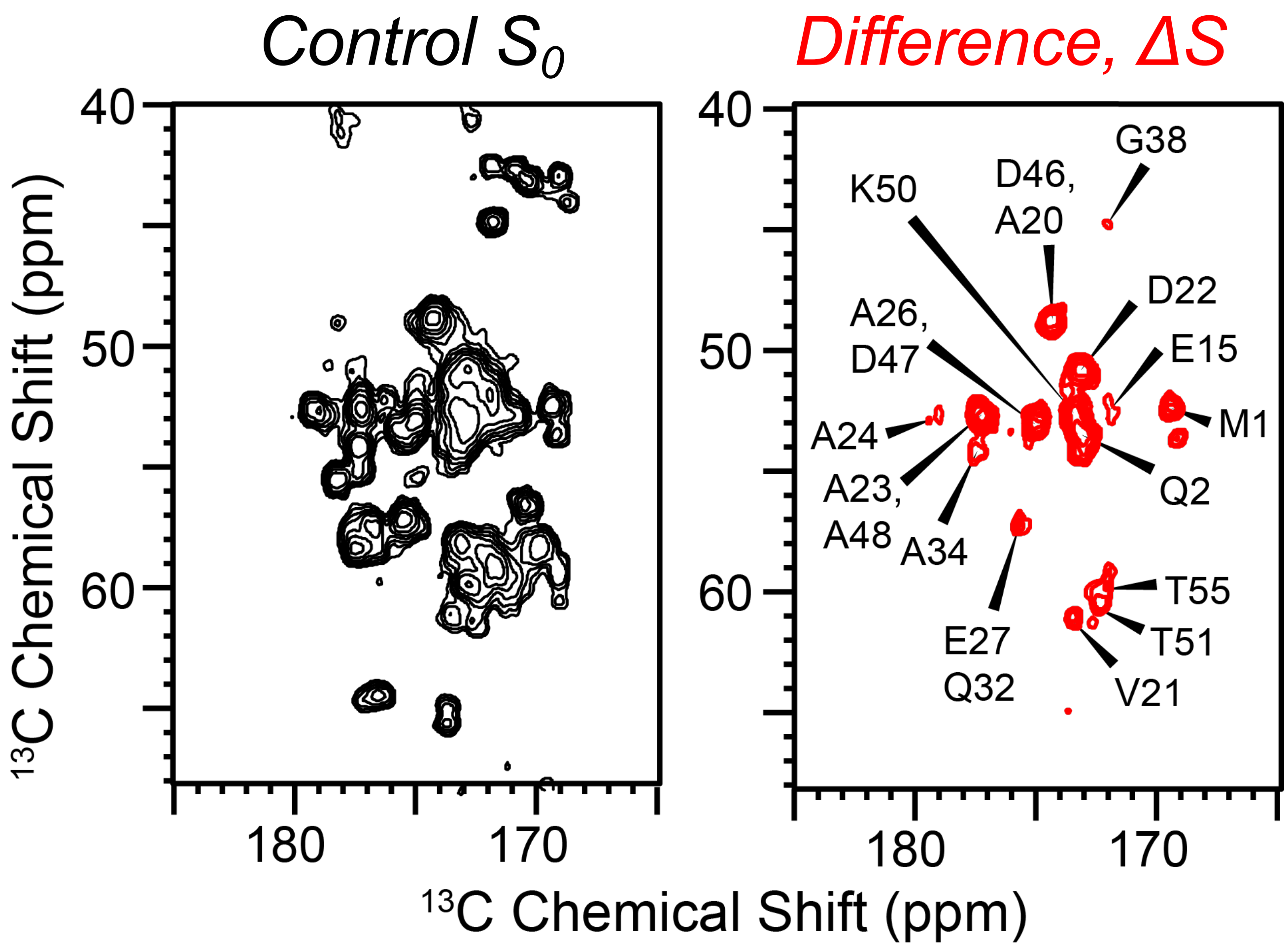

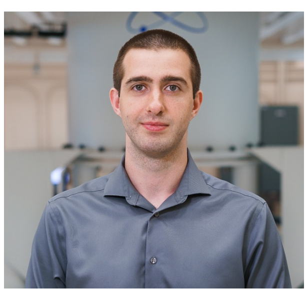

Alex Shcherbakov

Shcherbakov and Hong, ***J. Biomol. NMR***, 71, 31 (2018).

^{13}C-^{19}F Distances: 3F-Tyr GB1

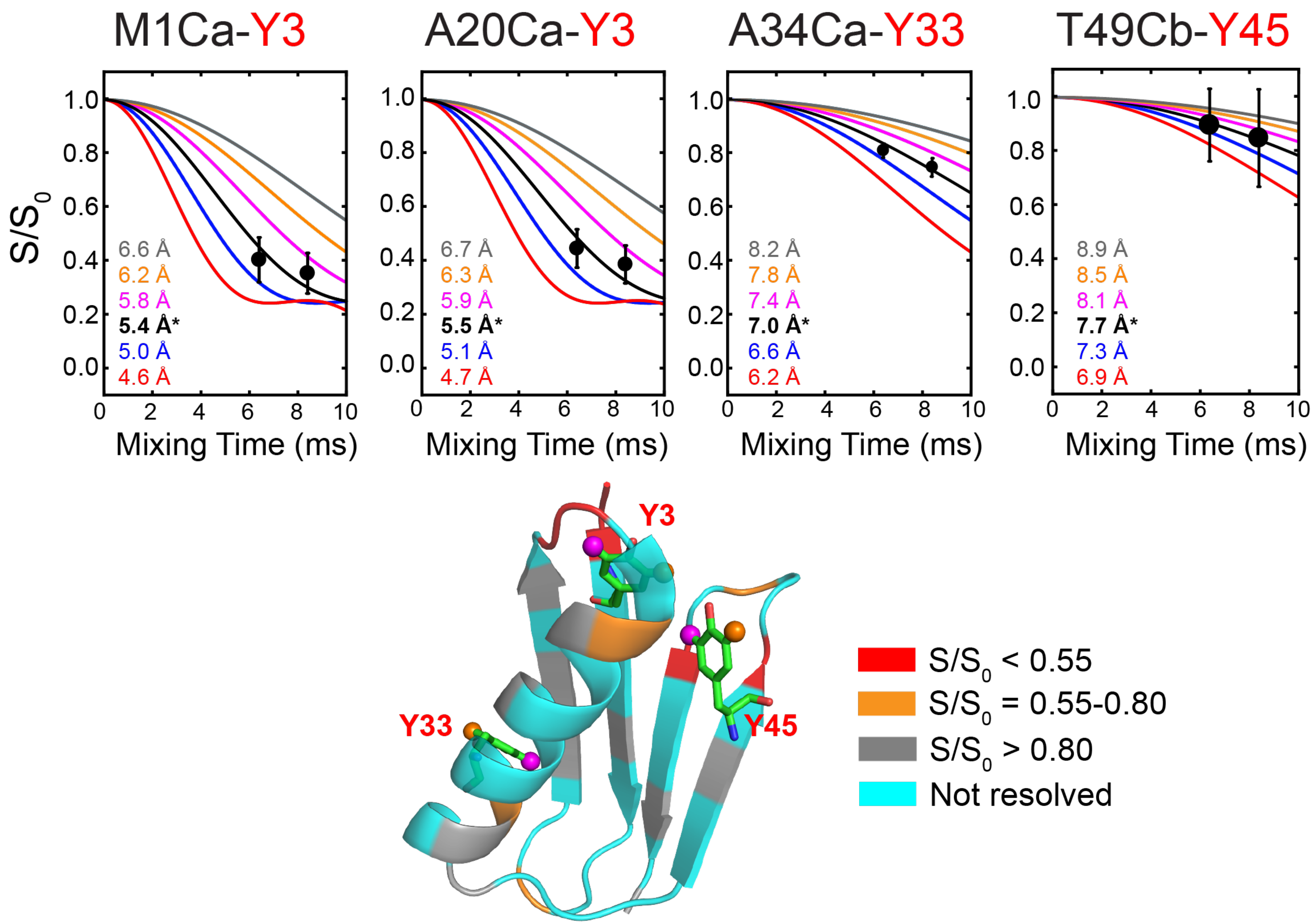

Shcherbakov and Hong, ***J. Biomol. NMR***, 71, 31 (2018).

^{13}C-^{19}F REDOR: 1 Å Accuracy for 1 nm Distances

5F-Trp GB1

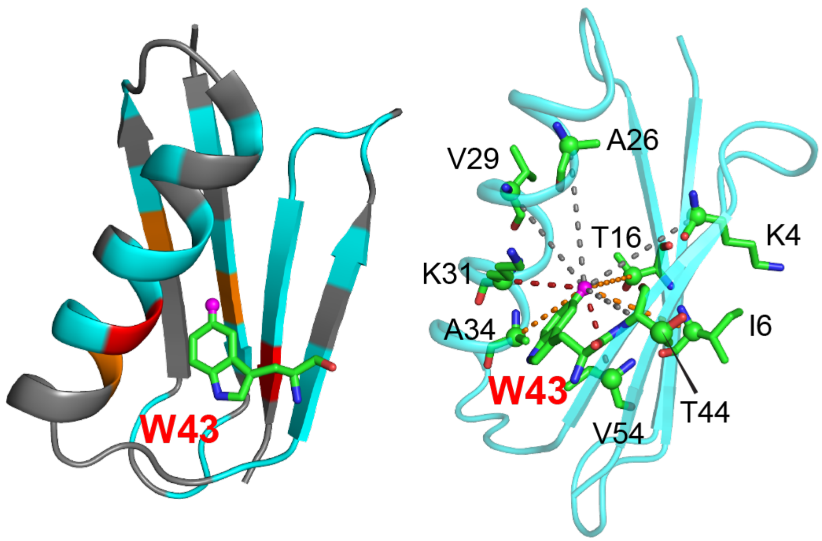

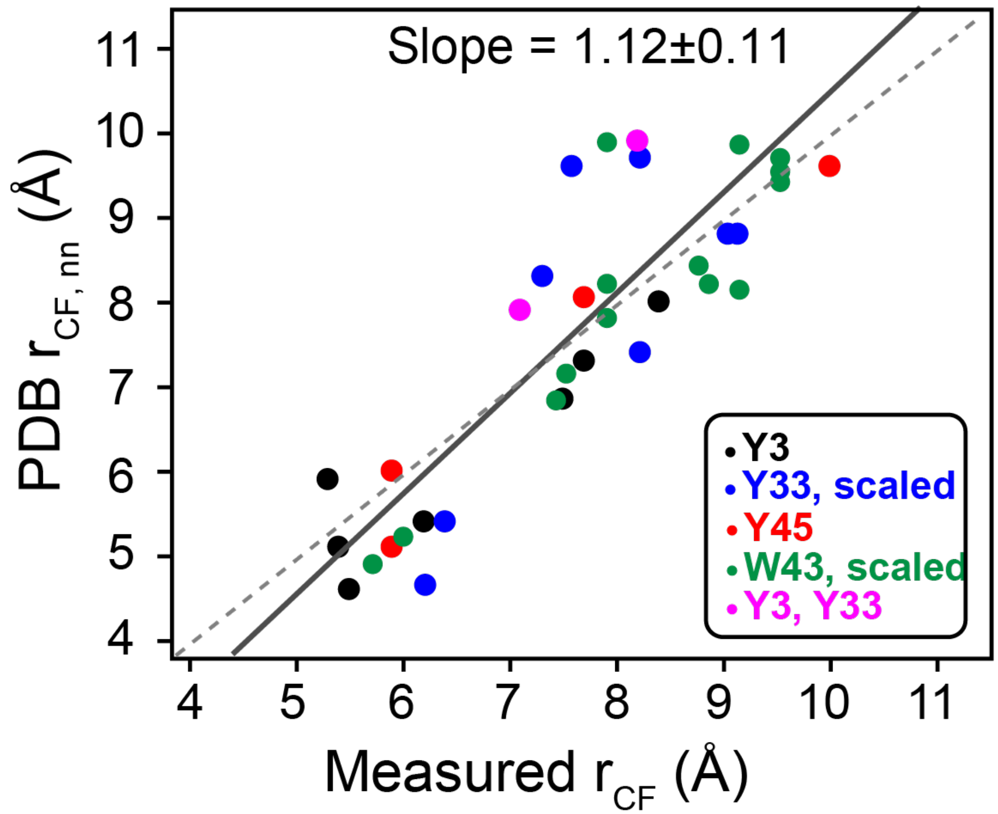

3F-Tyr GB1

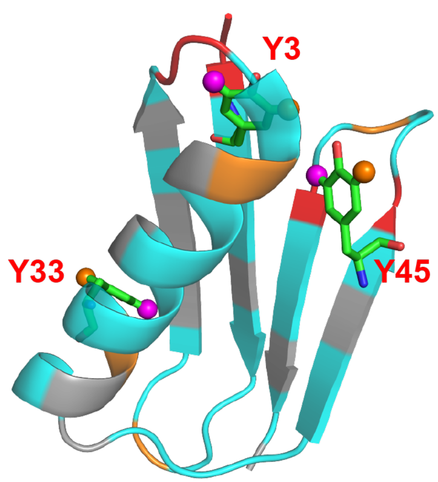

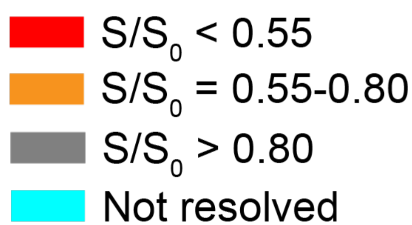

Shcherbakov and Hong, ***J. Biomol. NMR***, 71, 31 (2018).

^{19}F Chemical Shift Anisotropy: Residual Motion

3F-Tyr-GB1

12 kHz MAS

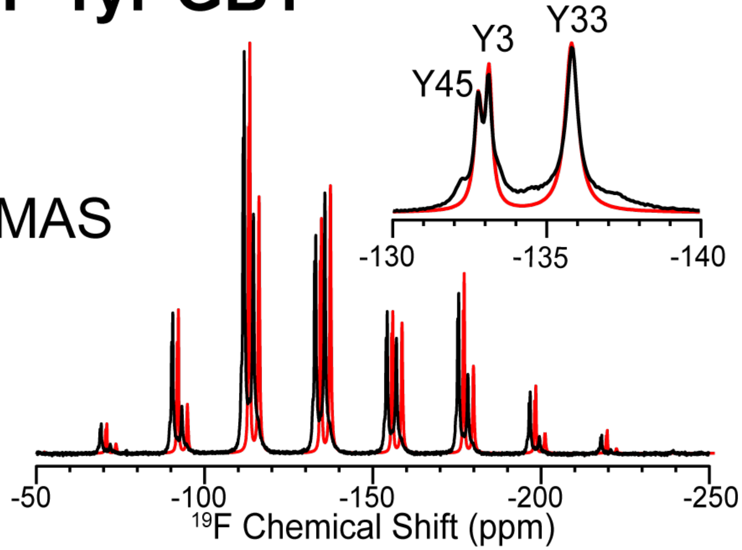

(δ_{iso}, δ_{CSA}, η)

3F-Y45: (-132.8 ppm, -75 ppm, 0.4)

3F-Y3: (-133.1 ppm, -76 ppm, 0.4)

3F-Y33: (-135.8 ppm, -58 ppm, 0.4)

— ***Experimental***

— ***Best-fit simulation***

5F-Trp-GB1

7 kHz MAS

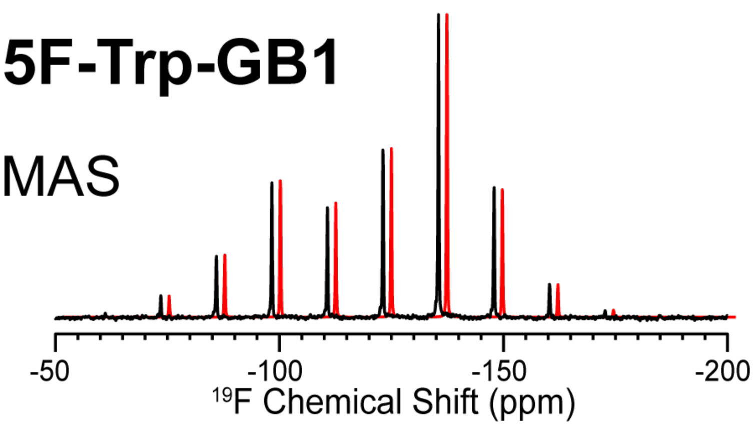

5F-W43: (-123.1 ppm, +46.6 ppm, 0.5)

2D hNH Resolved ^{1}H-^{19}F REDOR

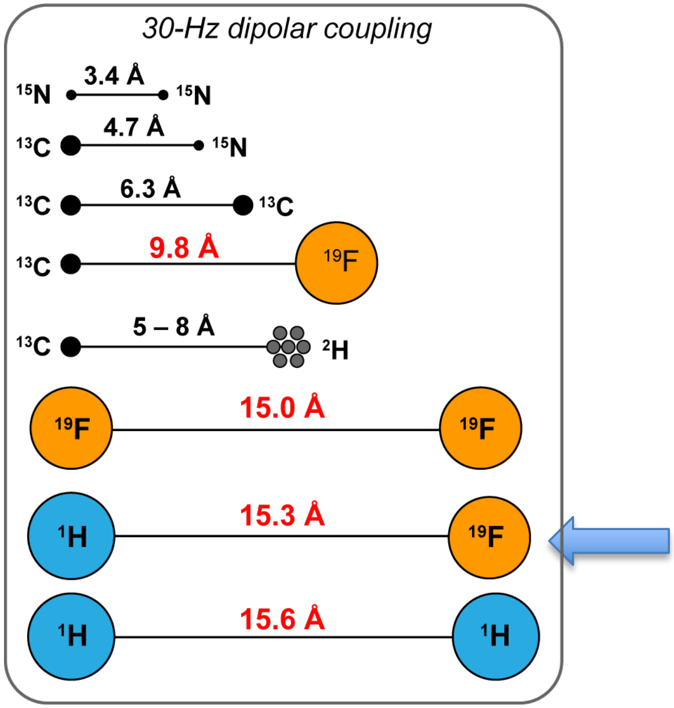

- Requires ^{13}C, ^{15}N, ^{2}H-labeled protein, back exchange to obtain H^{N}
- ^{19}F either recombinantly incorporated into the protein or provided by a ligand

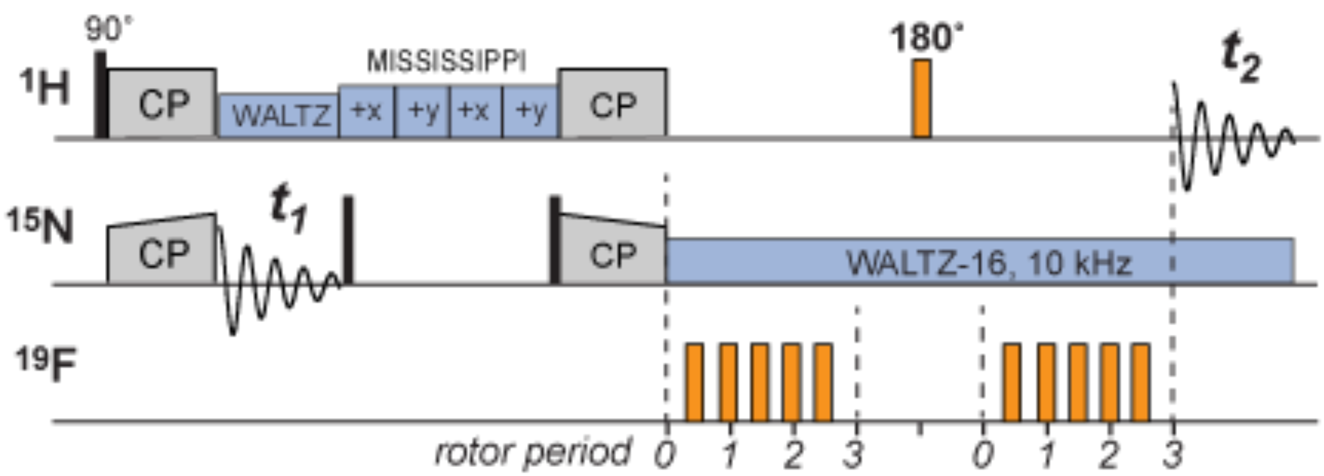

Shcherbakov et al. ***J. Phys. Chem***. 123, 4387 (2019).

Rapid Measurement of ^{1}H-^{19}F Distances

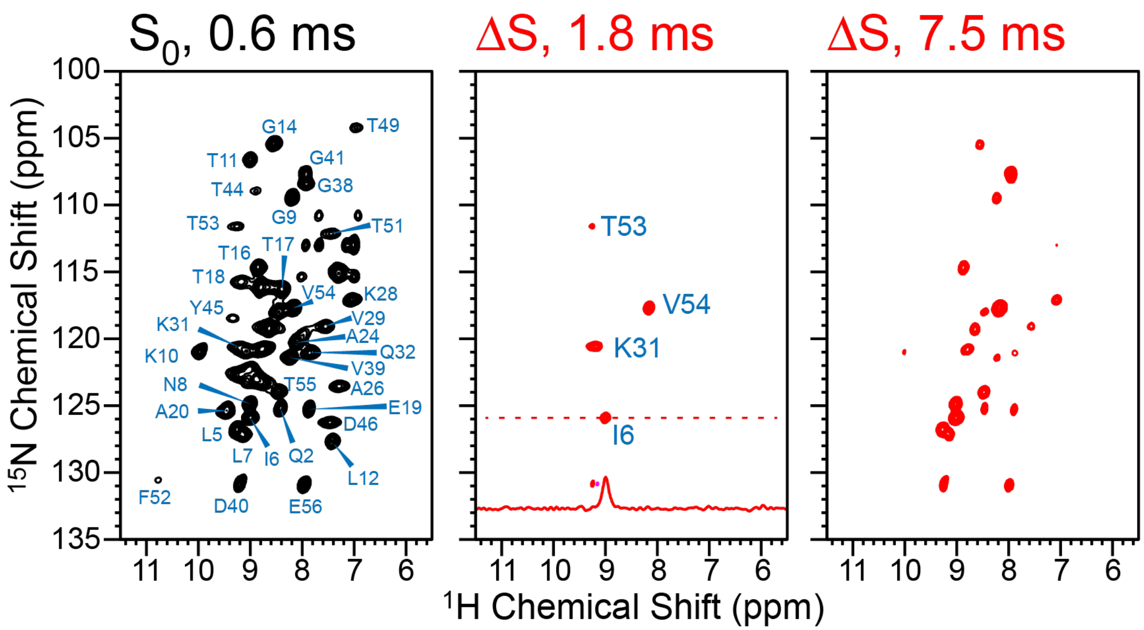

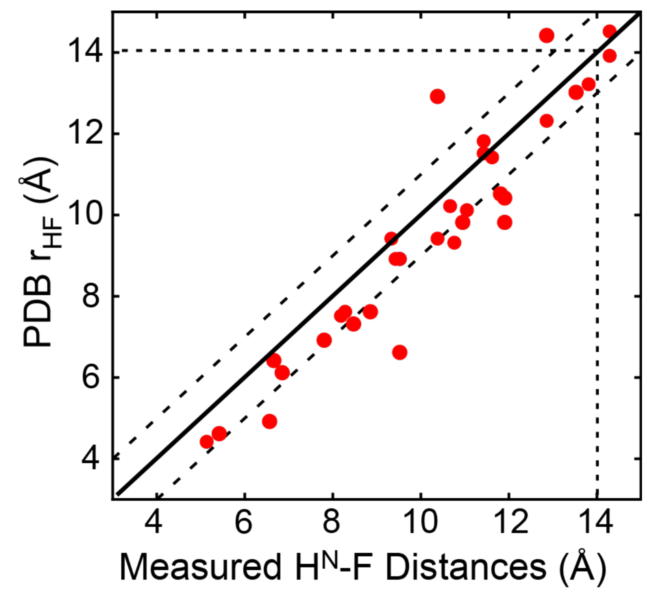

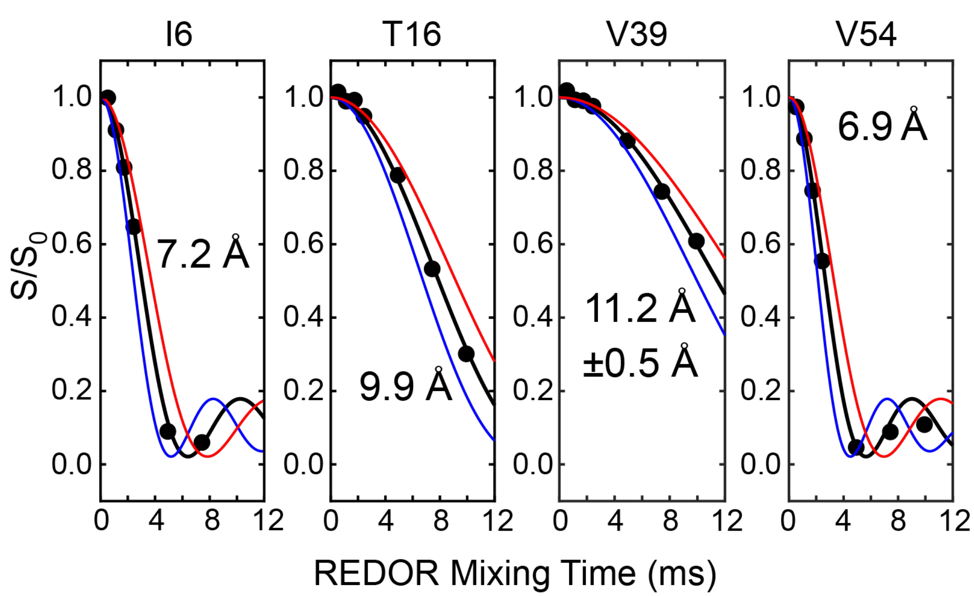

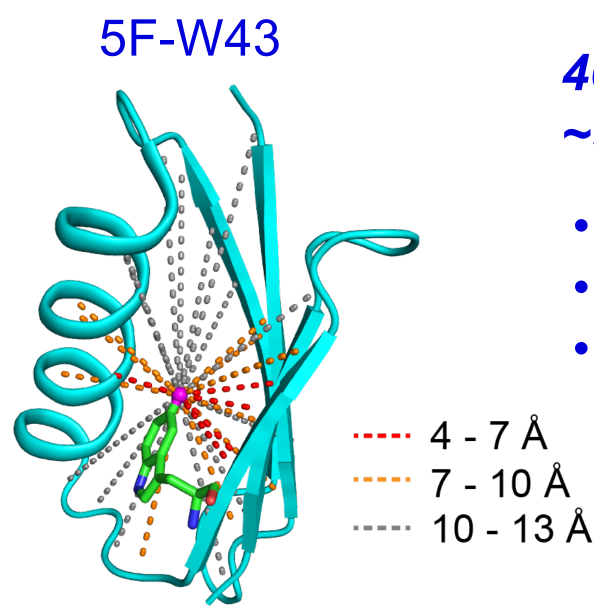

40 kHz MAS, ~3 hr / 2D

- ***Fast***
- ***Long***
- ***Precise***

Shcherbakov et al., ***JPC***, 2019.

Distance Precision and Accuracy

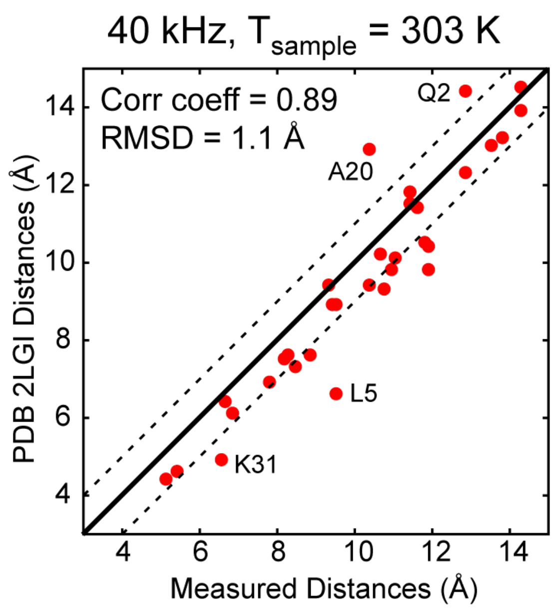

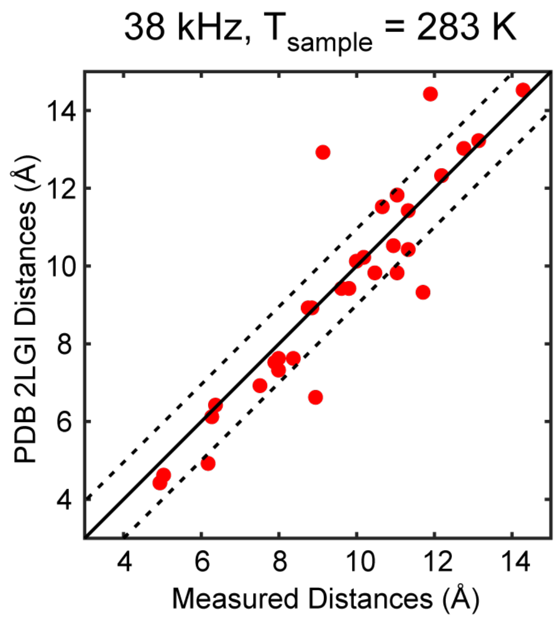

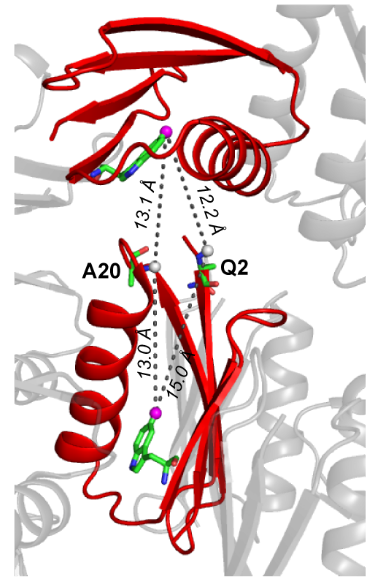

1.5 x 1.4 x 2.9 nm^3

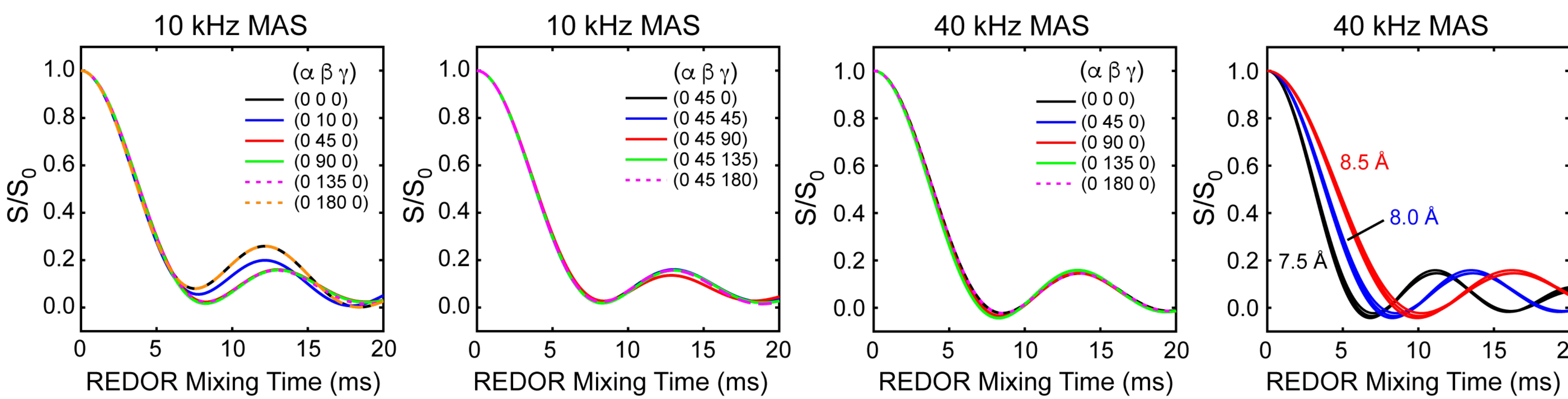

REDOR dephasing at fast MAS is independent of ^{19}F CSA tensor orientation.

Shcherbakov et al. ***J. Phys. Chem***. 123, 4387 (2019).

^{19}F-Enhanced ssNMR for Structure Determination

SARS-CoV-2 envelope protein

closed

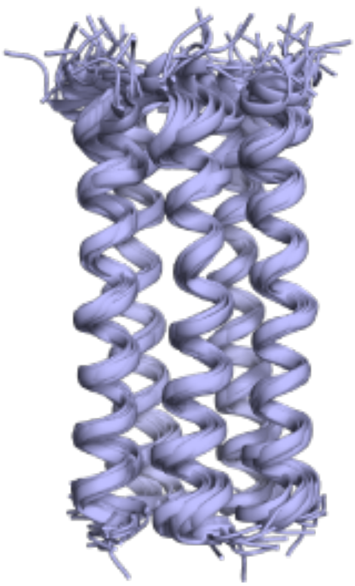

open

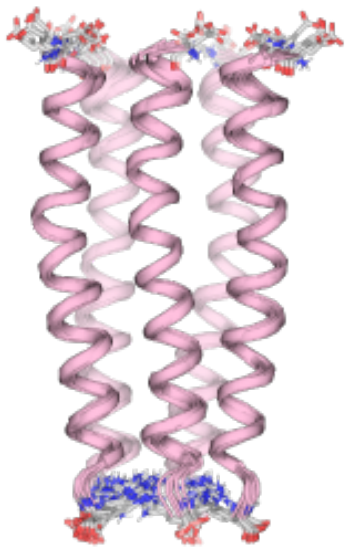

Multidrug-resistance transporter EmrE

High pH

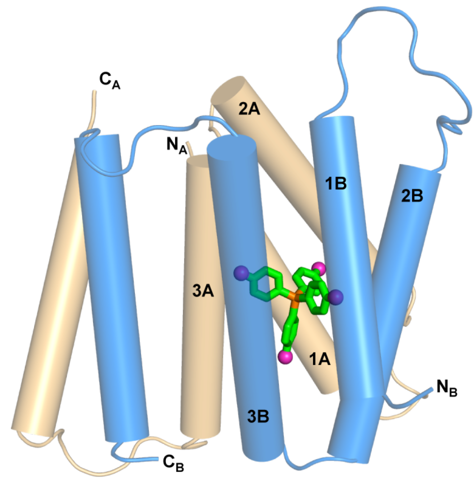

Low pH

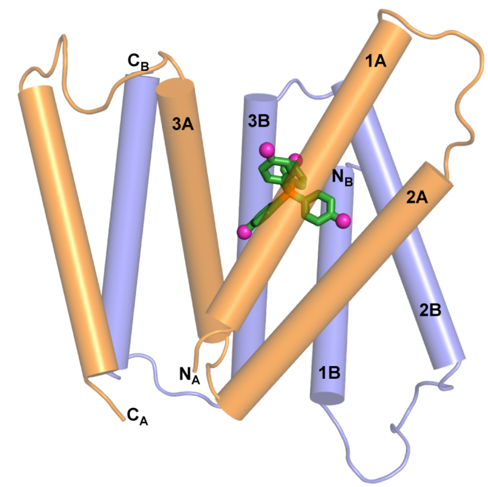

PET tracer binding to Aβ

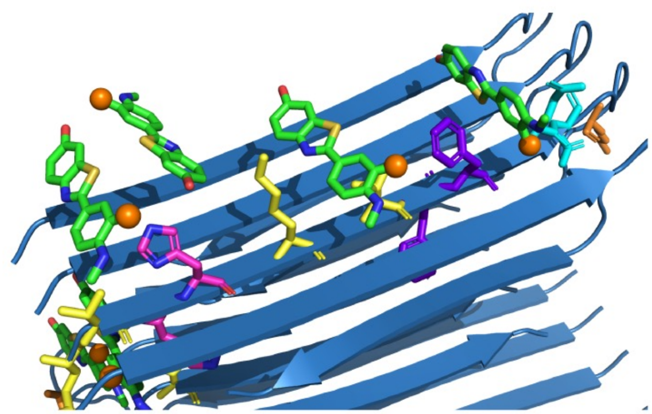

ETM is Well Ordered in Lipid Bilayers

ERGIC membrane:
POPC : POPE : PI : POPS : Chol
(45 : 20 : 13 : 7 : 15)

pH 7.5

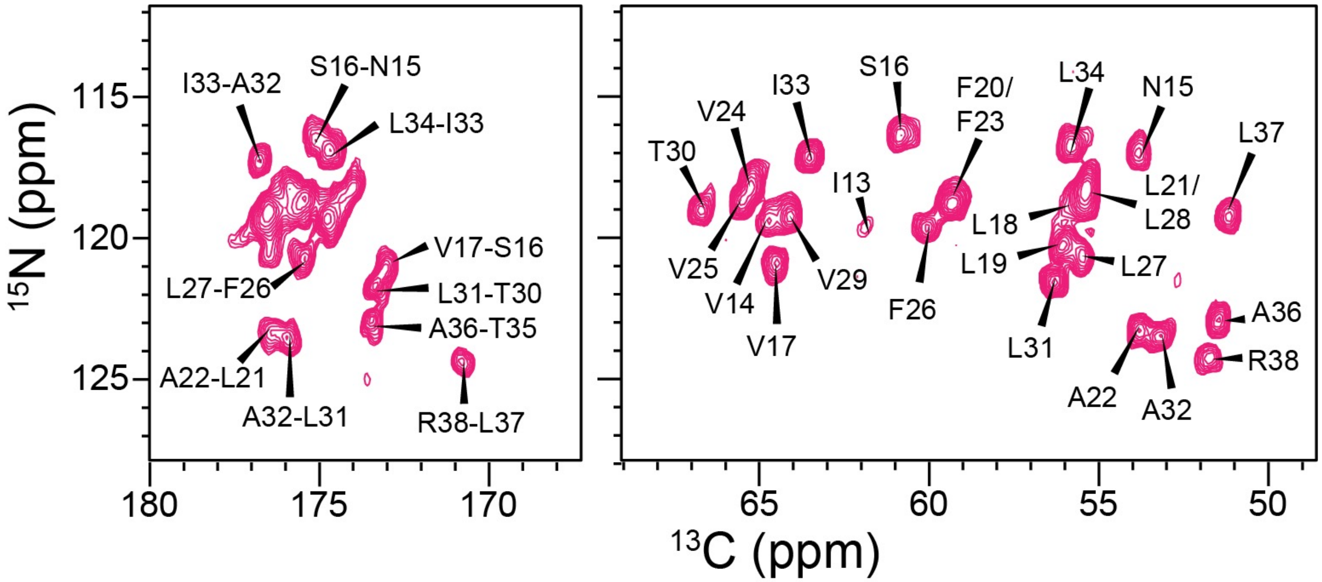

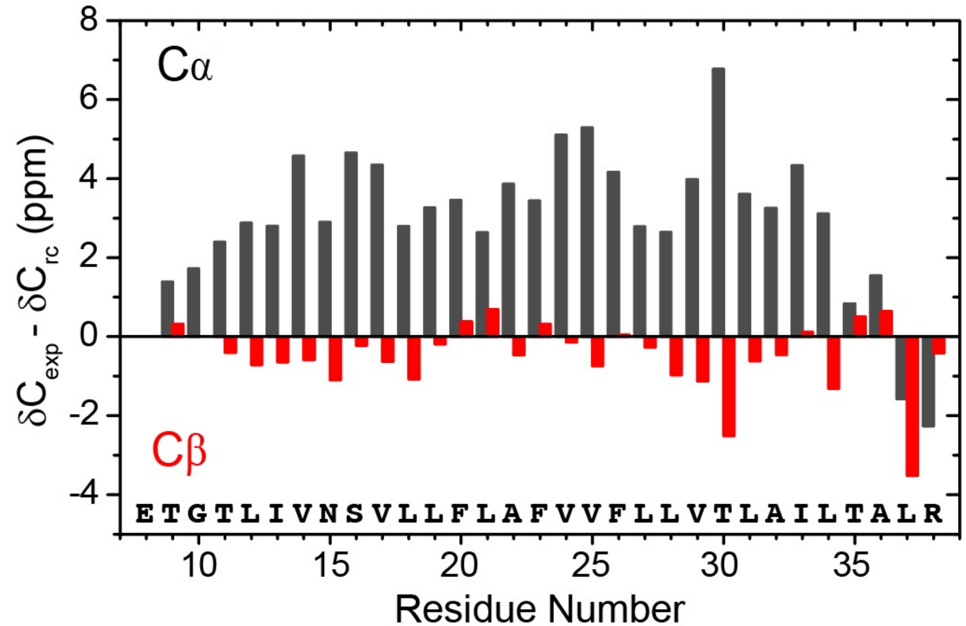

Venkata Shiva Mandala, Matt McKay

Interhelical Distances From ^{13}C-^{19}F REDOR

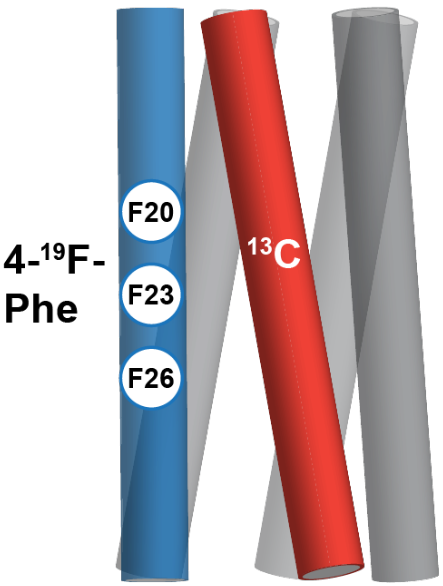

10.3 ms REDOR mixing, 14 kHz MAS

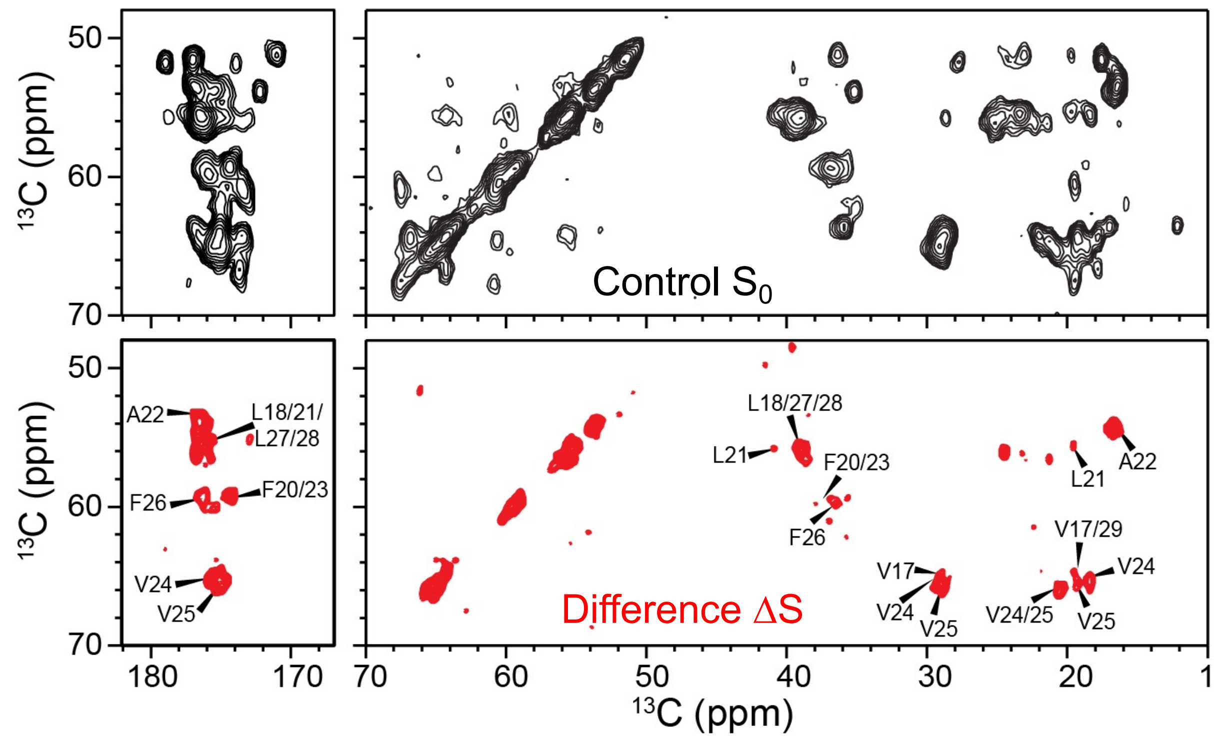

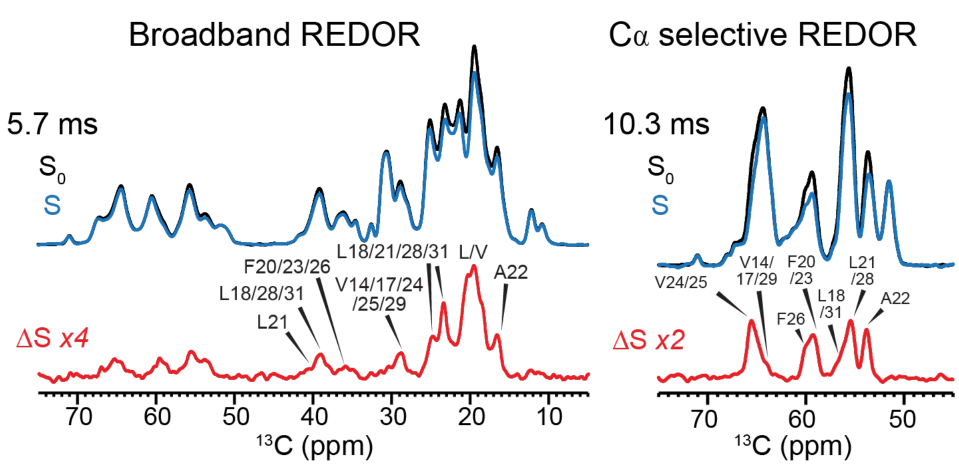

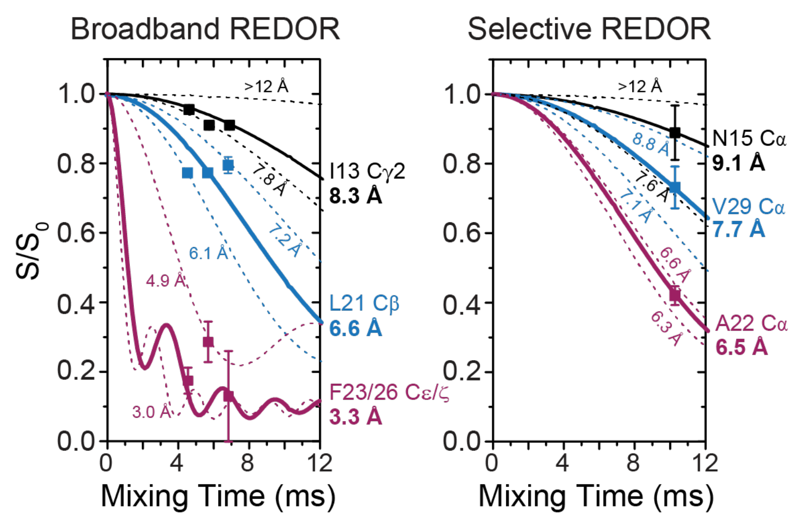

Pore-Facing versus Lipid-Facing Residues

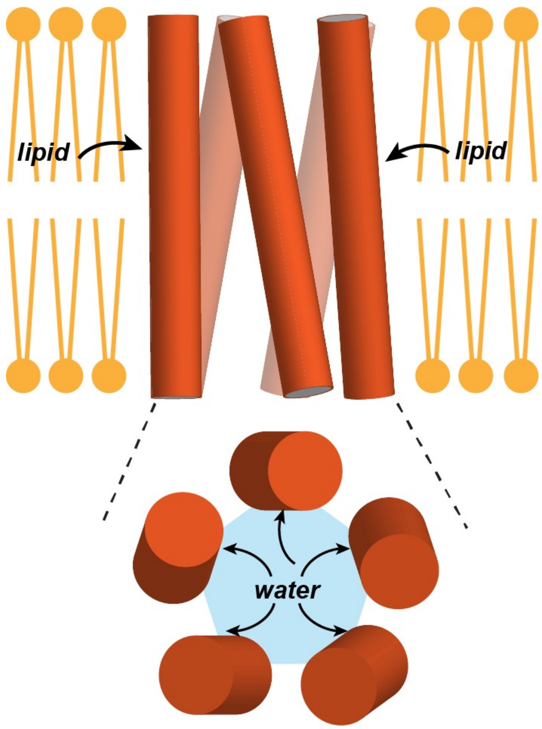

Water-transferred intensities

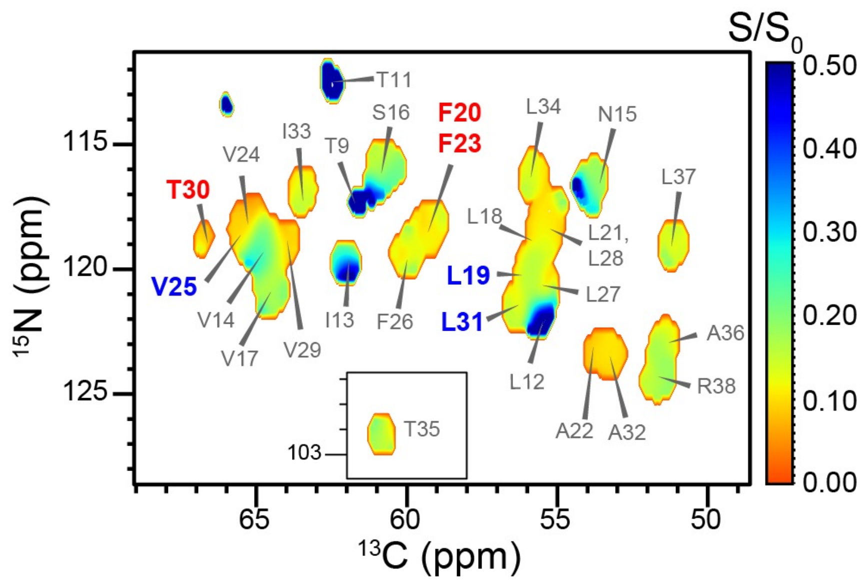

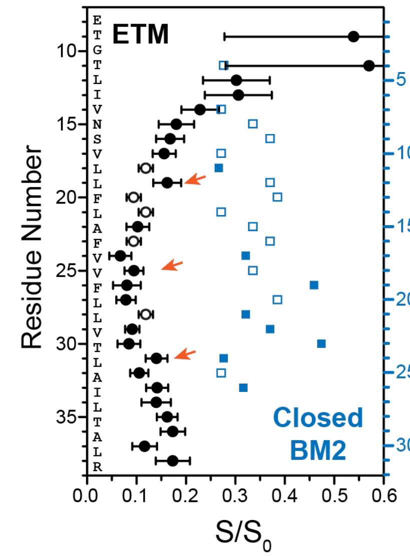

Lipid-transferred intensities

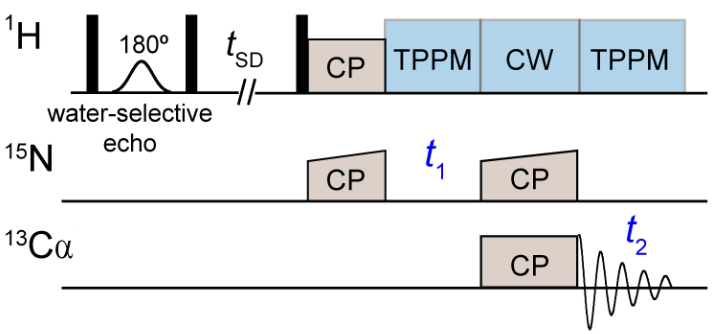

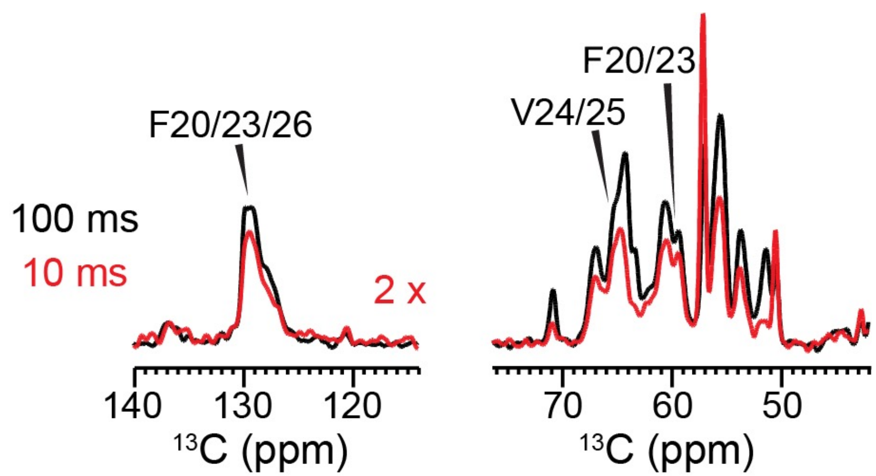

Mandala, McKay, Shcherbakov, Dregni, Kolocouris & Hong, ***Nat. Struc. Mol. Biol***, 2020.

Structure of the Closed ETM in Lipid Bilayers

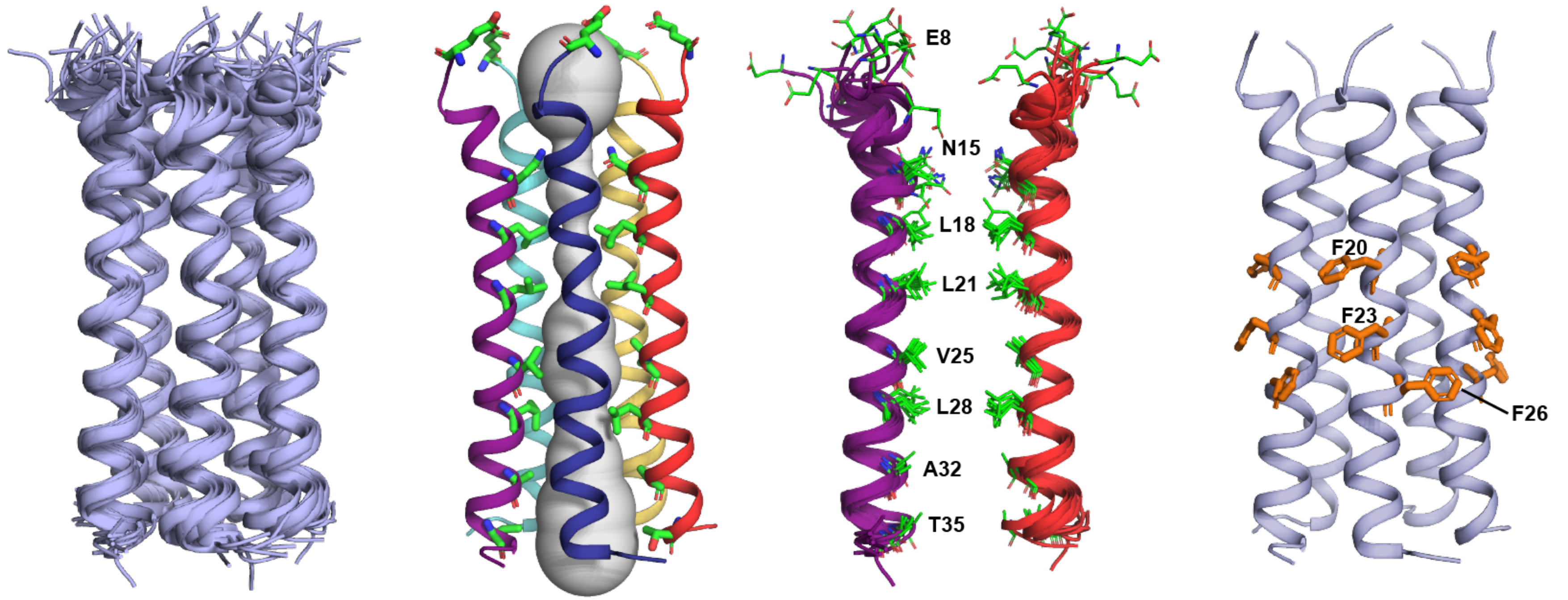

RMSD: 2.1 Å
PDB: 7K3G

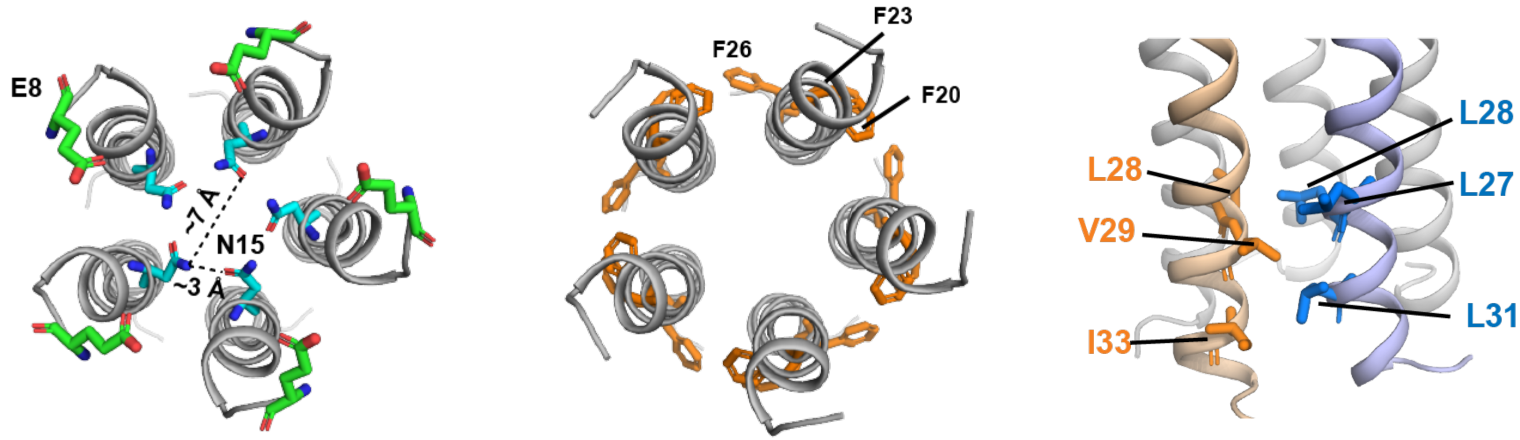

Shiva Mandala

Mandala, McKay, Shcherbakov, Dregni, Kolocouris & Hong, ***Nat. Struc. Mol. Biol***, 2020.

EmrE: a Bacterial Transporter

Couples proton transport with drug export to cause multidrug resistance

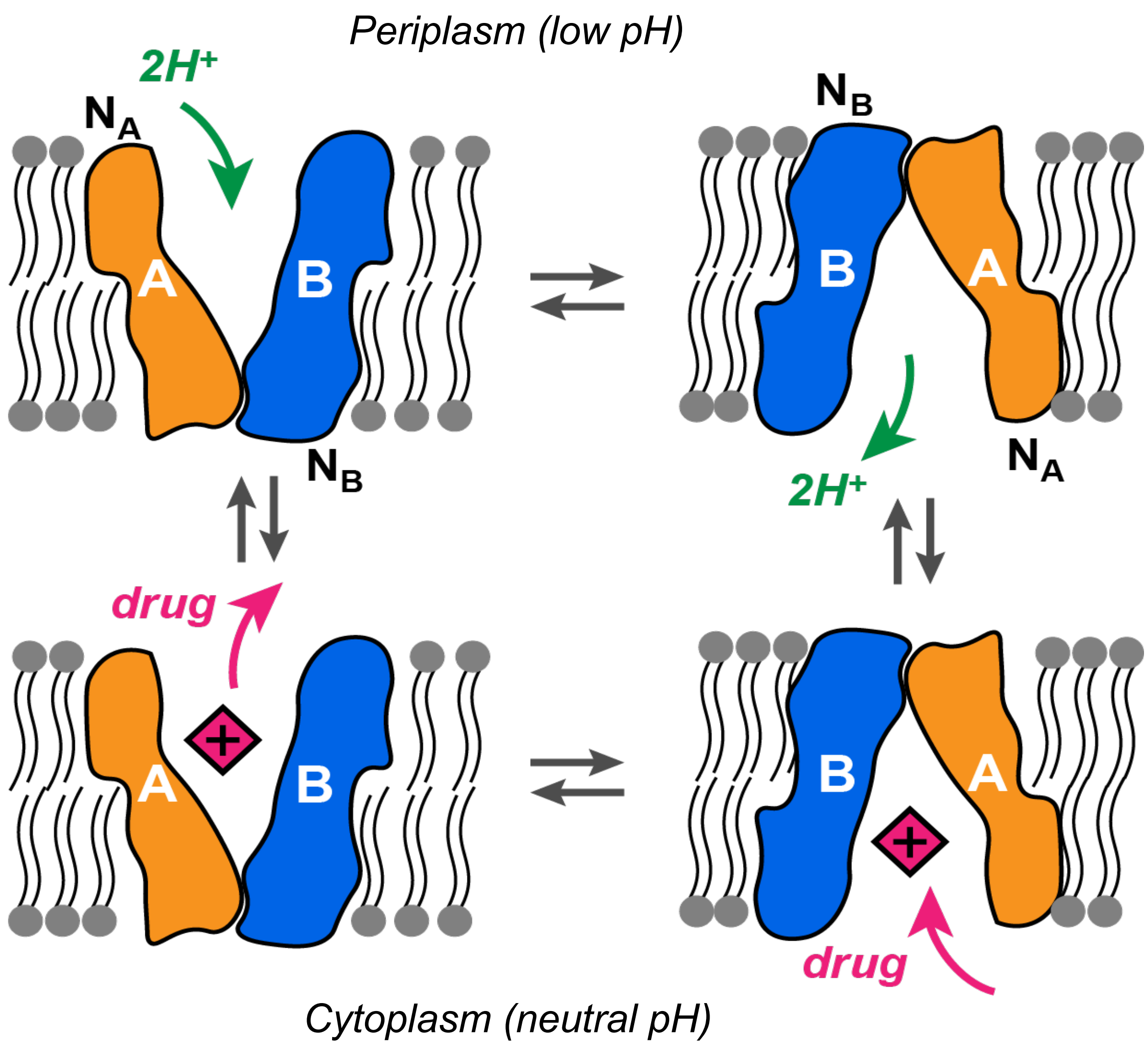

Prior NMR studies: **Katie Henzler-Wildman,** Nate Traaseth, Clemens Glaubitz

Backbone Crystal Structure & Sidechain MD

3.8 Å crystal structure of the backbone

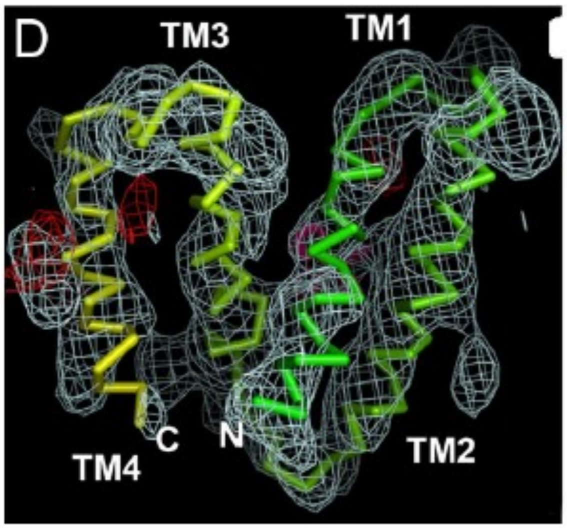

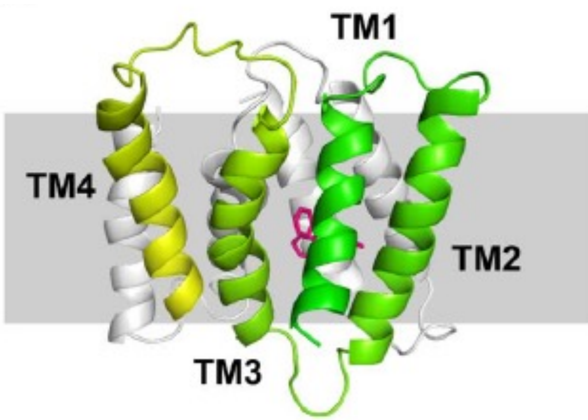

Chen…Chang, ***PNAS***, 2007.

MD simulations of the active site

Ribbons: MD

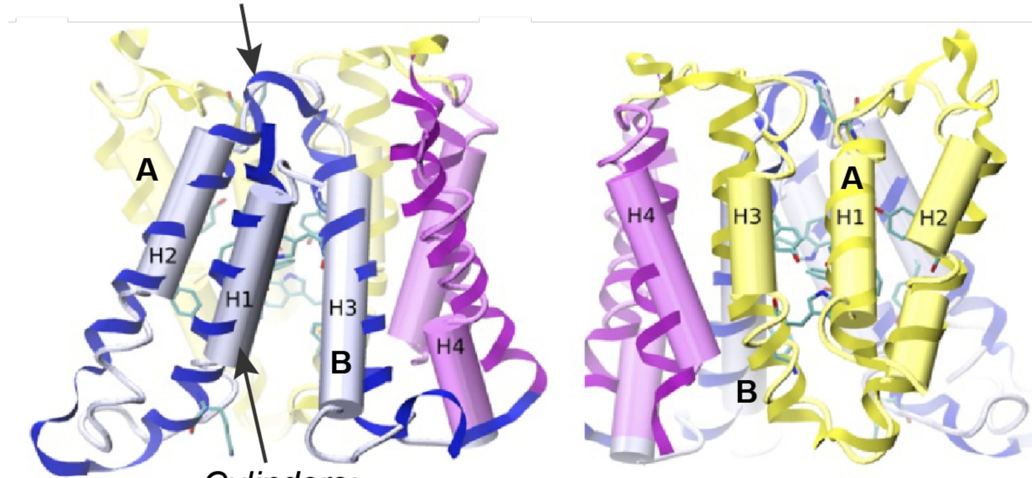

Cylinders: xtal struc.

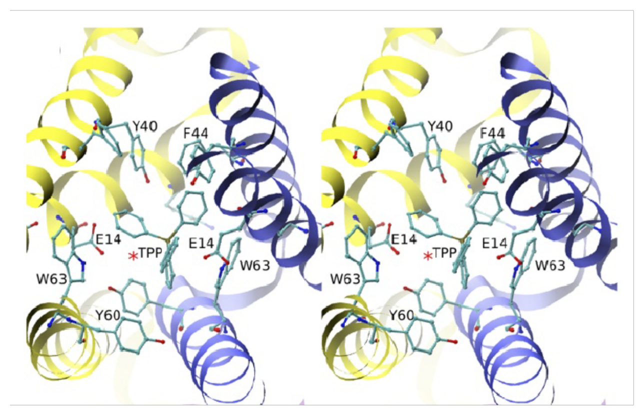

Ovchinnikov…Karplus, ***PNAS***, 2018.

^{19}F NMR Spectra of the Substrate

F_4-TPP$^+$

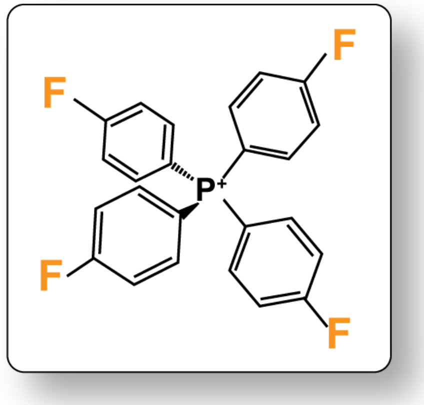

In DMPC bilayers,
P : L = 1 : 25 (mole)

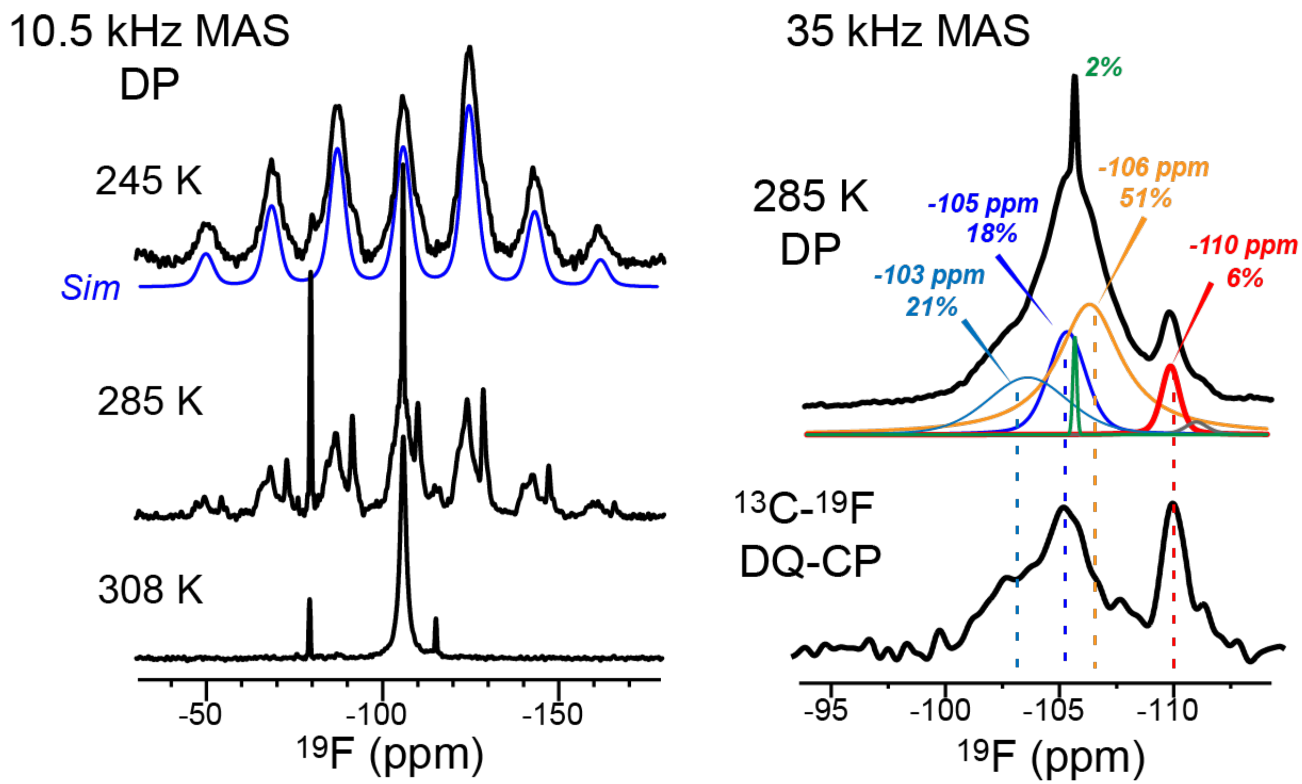

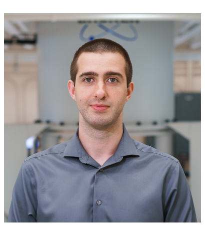

Alex Shcherbakov

Protein-Substrate H^N-F Distances

- CDN-labeled S64V-EmrE (Grant Hisao, Katie Henzler-Wildman)
- DMPC bilayers, **pH 5.8**
- 38 kHz MAS

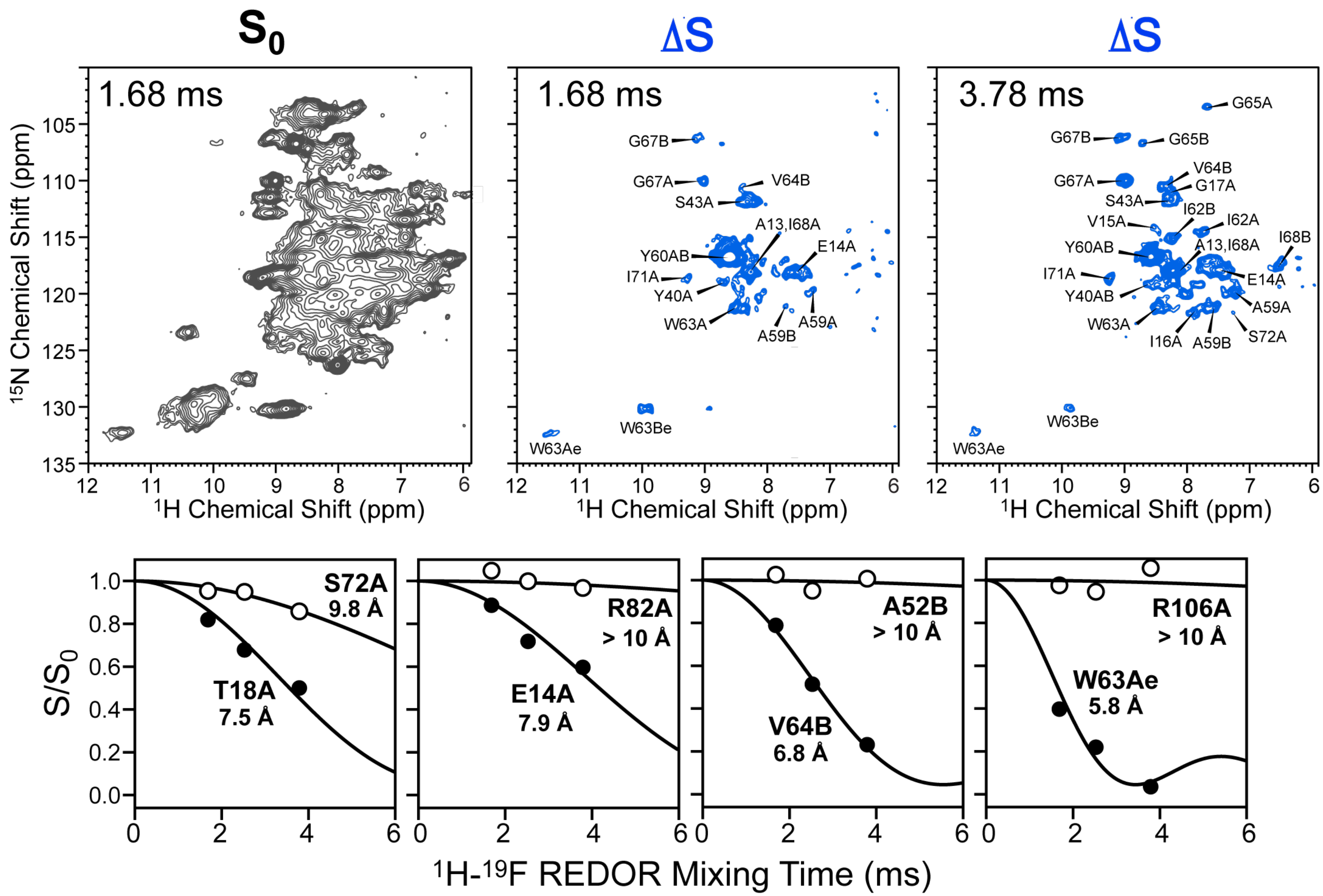

Shcherbakov, Hisao …Henzler-Wildman, Hong, ***Nature Comm.***, 2021.

TPP is Near TM1 and TM3 Helices

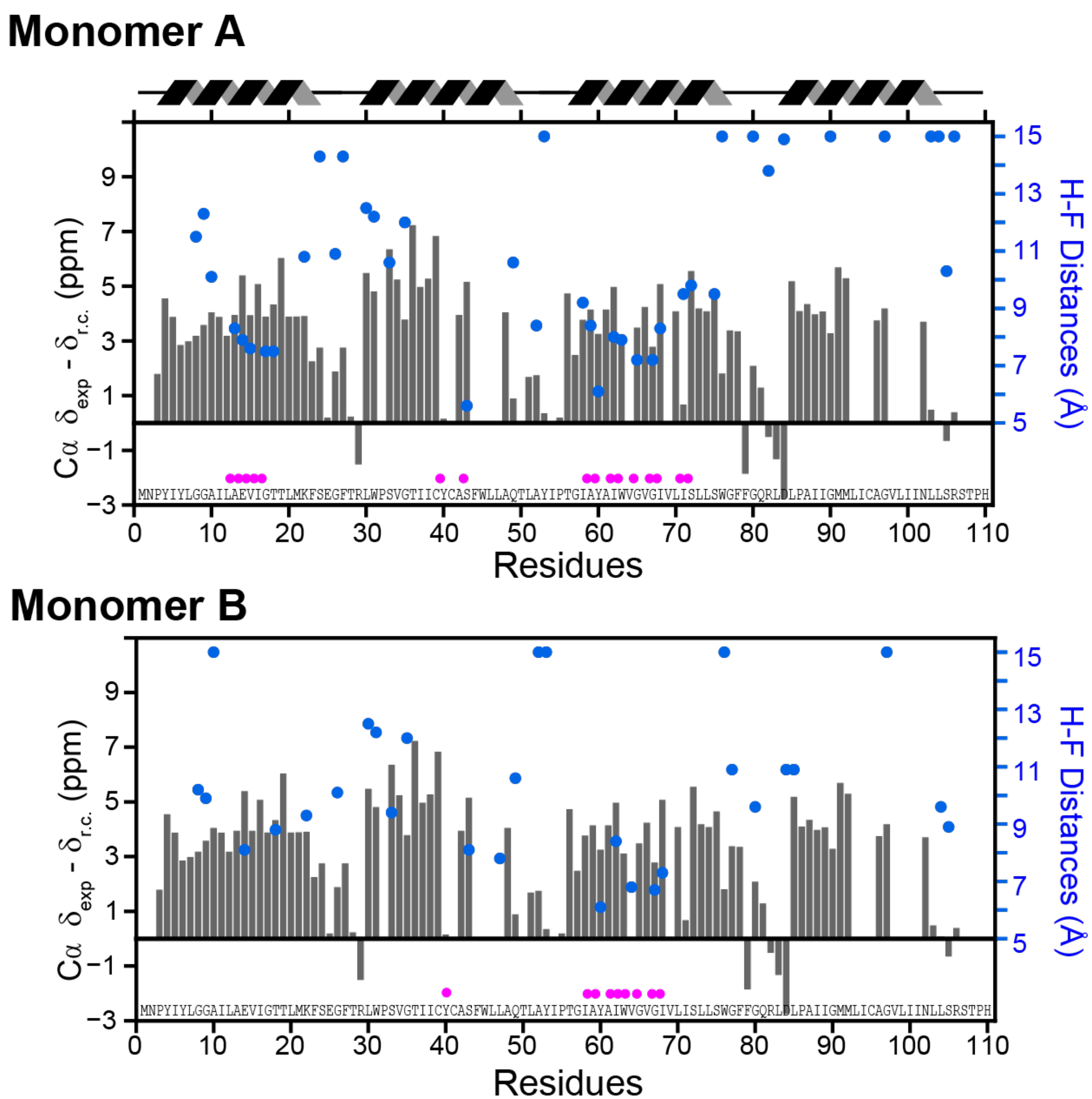

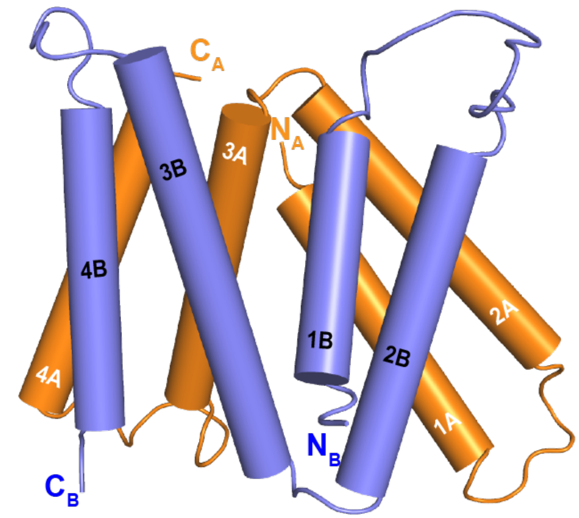

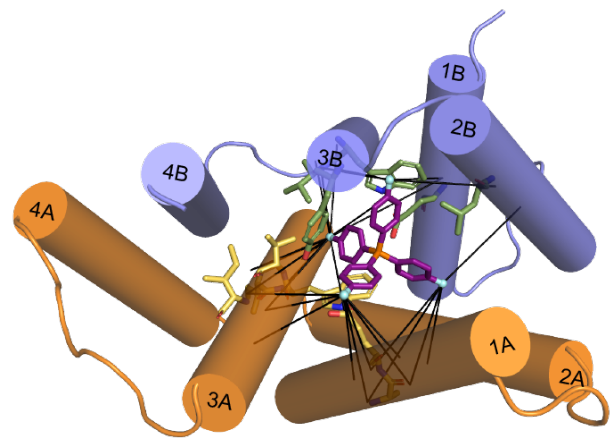

Shcherbakov, Hisao …Henzler-Wildman, Hong, ***Nature Comm.***, 2021.

Substrate-Bound Structure of EmrE at Acidic pH

- 72 H-F dipolar couplings
- 214 protein-drug H-F distances
- 186 pairs of (ϕ, ψ) angles
- 95 χ_1 torsion angles

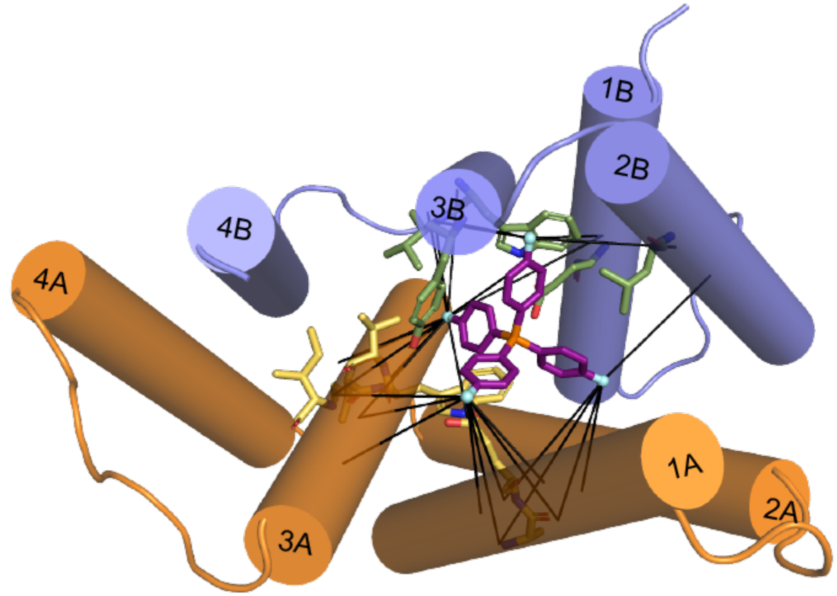

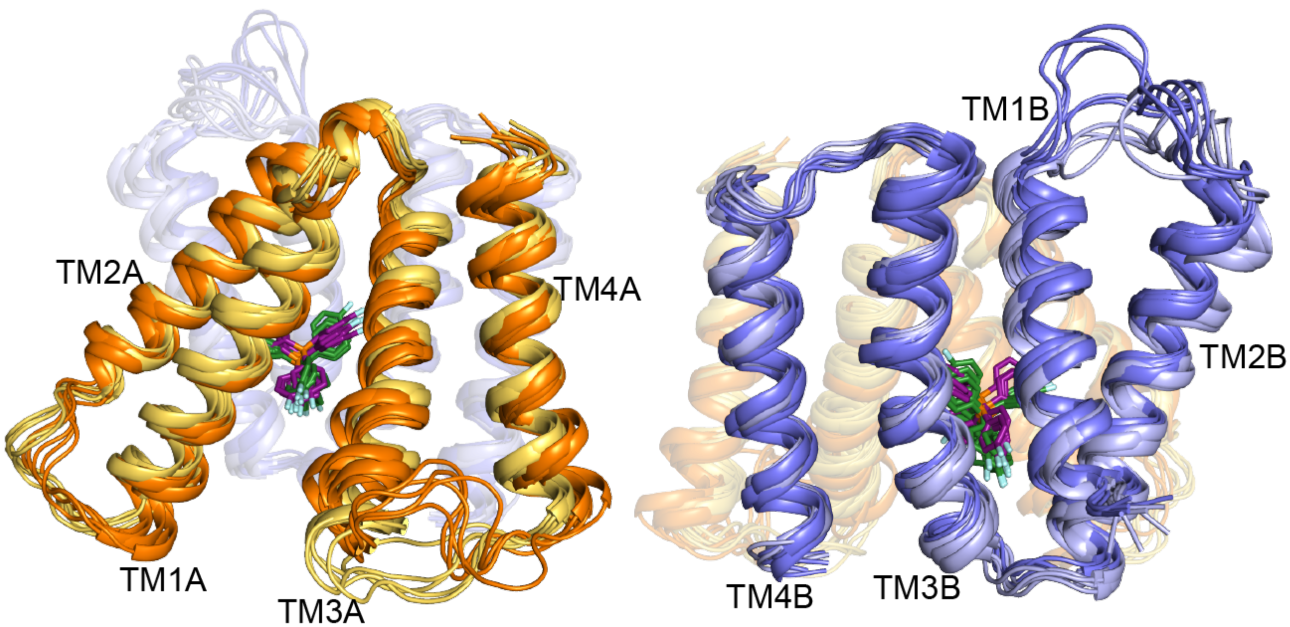

Alex Shcherbakov

Substrate-Bound Structure of EmrE at Acidic pH

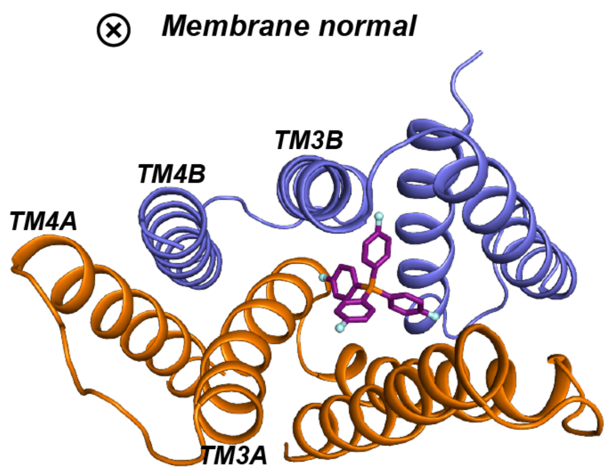

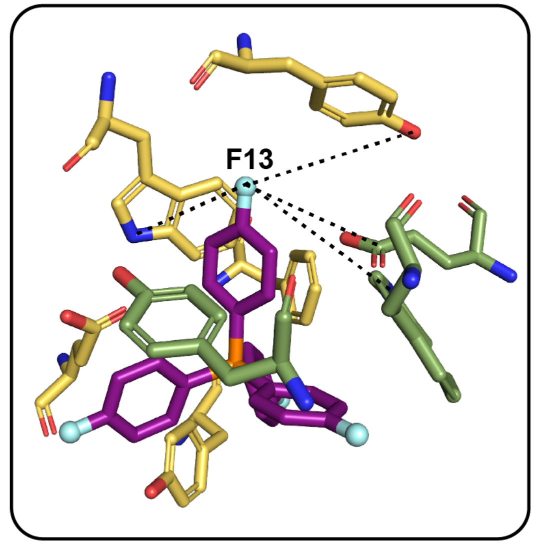

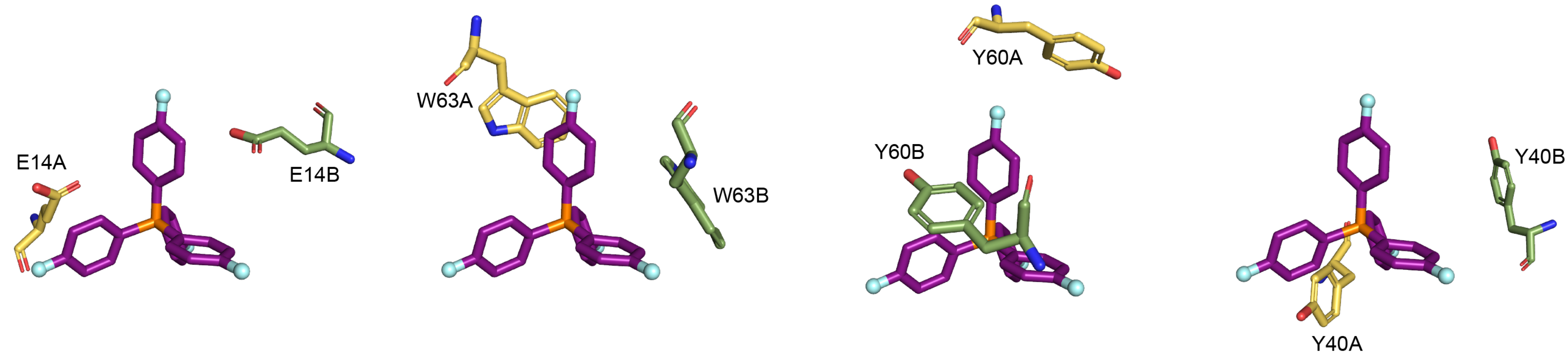

- TPP⁺ binds the two subunits asymmetrically
- Multivalent aromatic interactions
- Spacious binding site allows tetrahedral jumps

Shcherbakov, Hisao …Henzler-Wildman, Hong, ***Nature Comm***., 2021.

Fluorinated PET Tracers for Amyloid Imaging

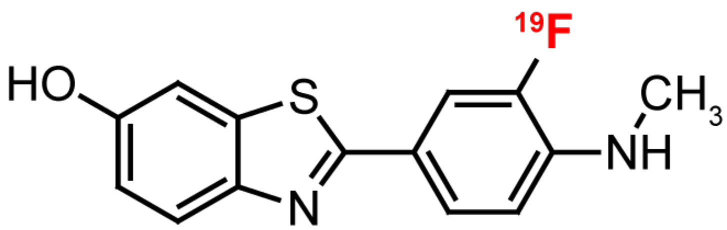

Flutemetamol

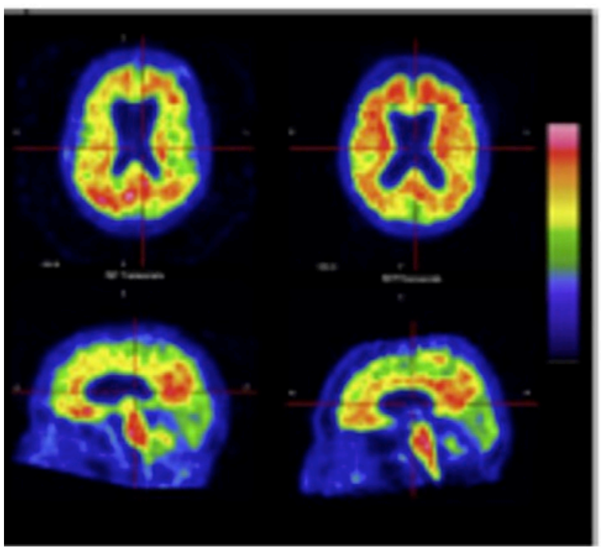

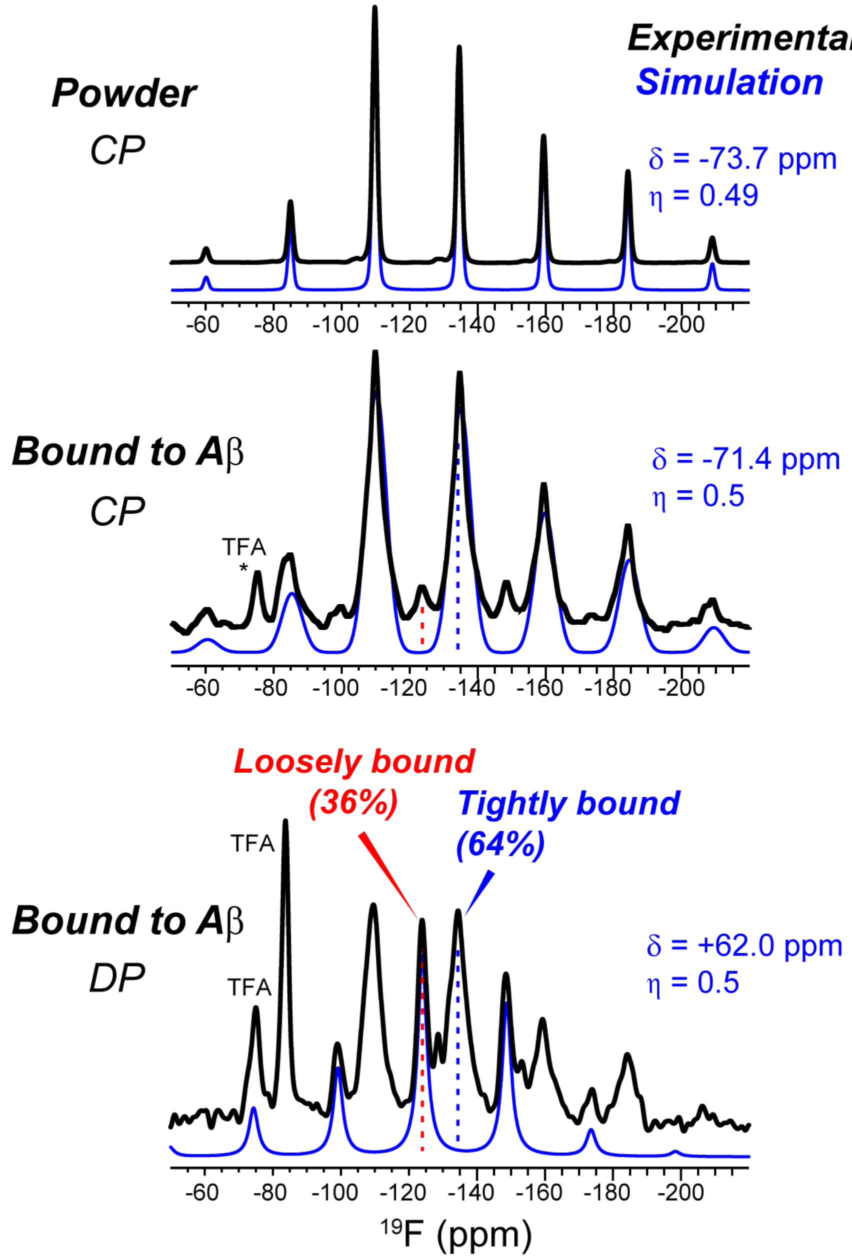

Duan et al. ***J. Am. Chem. Soc.***, 2022.

^{1}H-^{19}F REDOR Without Deuteration

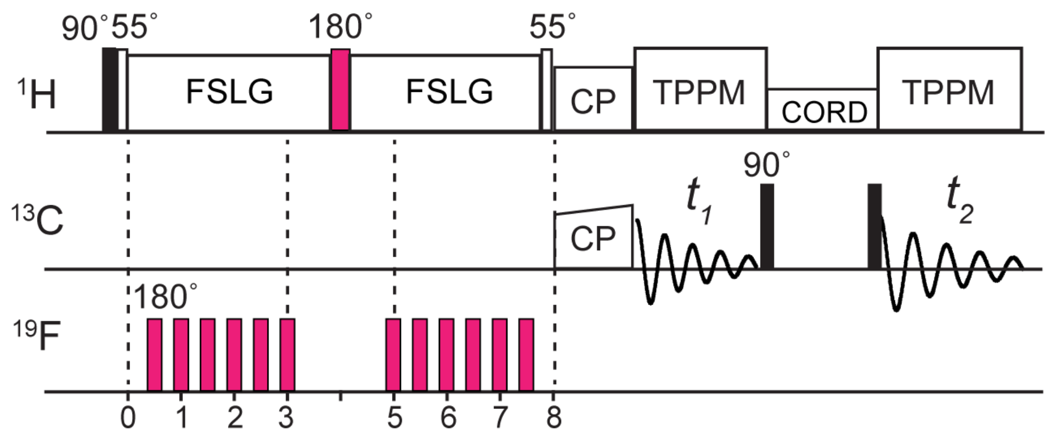

Aβ40 fibrils

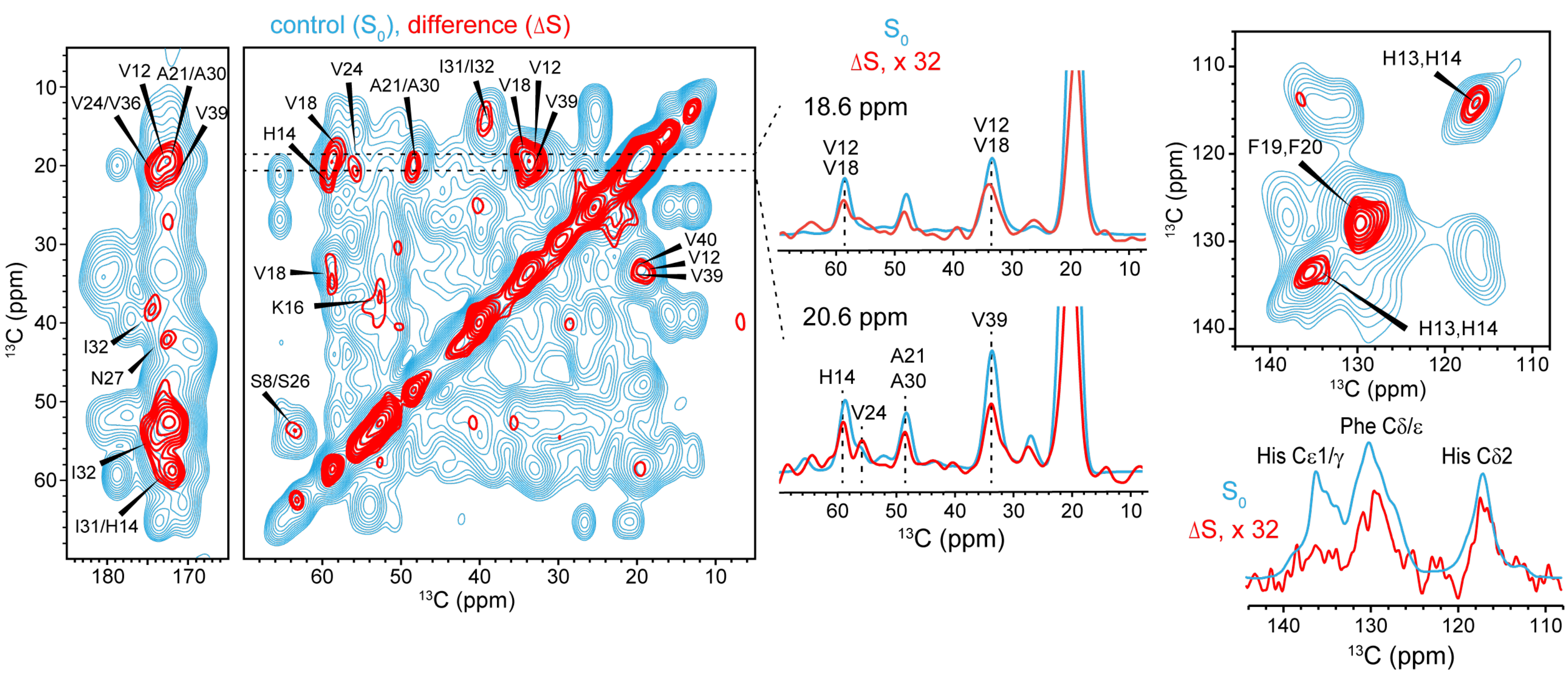

Duan et al. ***J. Am. Chem. Soc.***, 2022.

Flutemetamol Bind Doublet Motifs in Aβ: Polymorph Independence

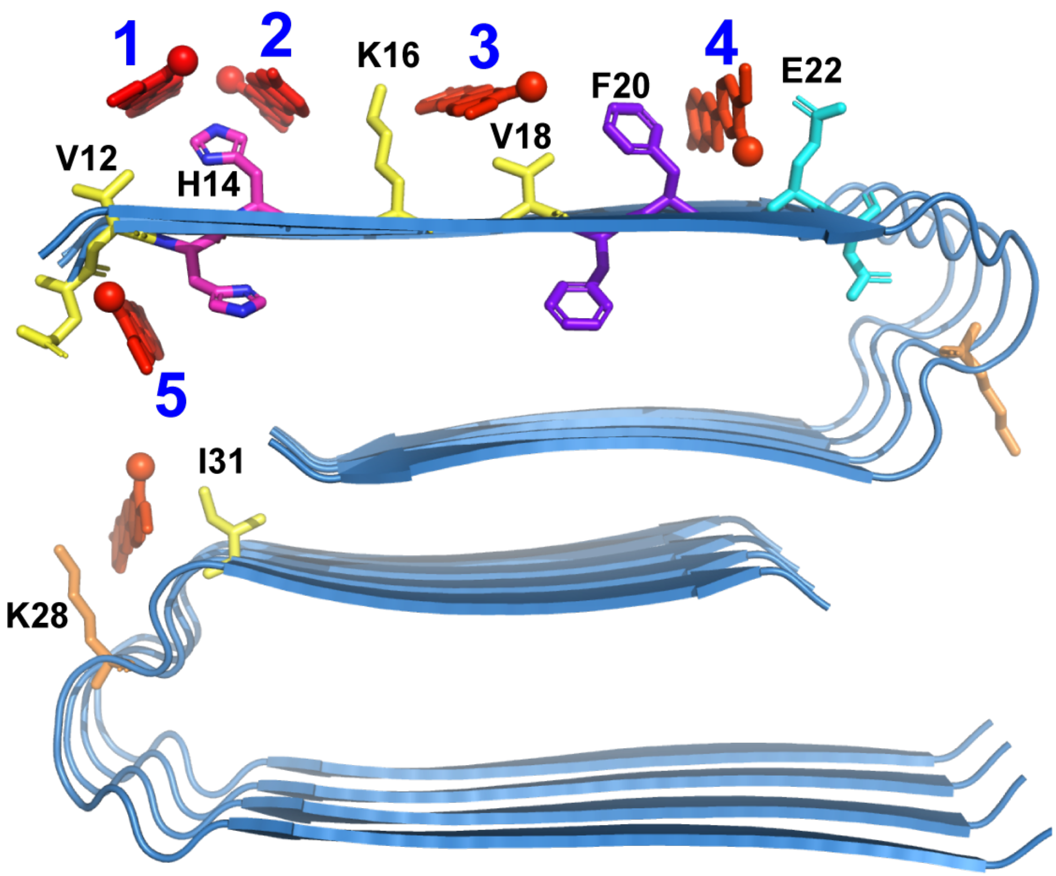

3 binding sites in Aβ fibrils: ^{12}VHH^{14}, ^{18}VFF^{20}, ^{39}VV^{40}

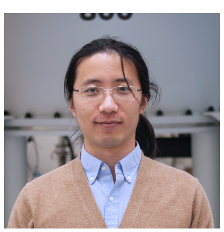

Pu Duan

Duan et al. ***J. Am. Chem. Soc.***, 2022.

Ligand Position Along the Fibril Axis

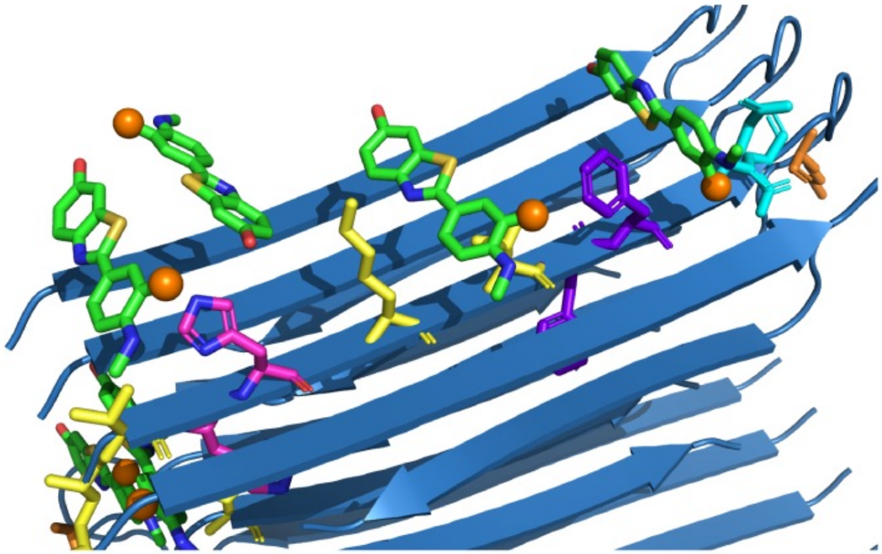

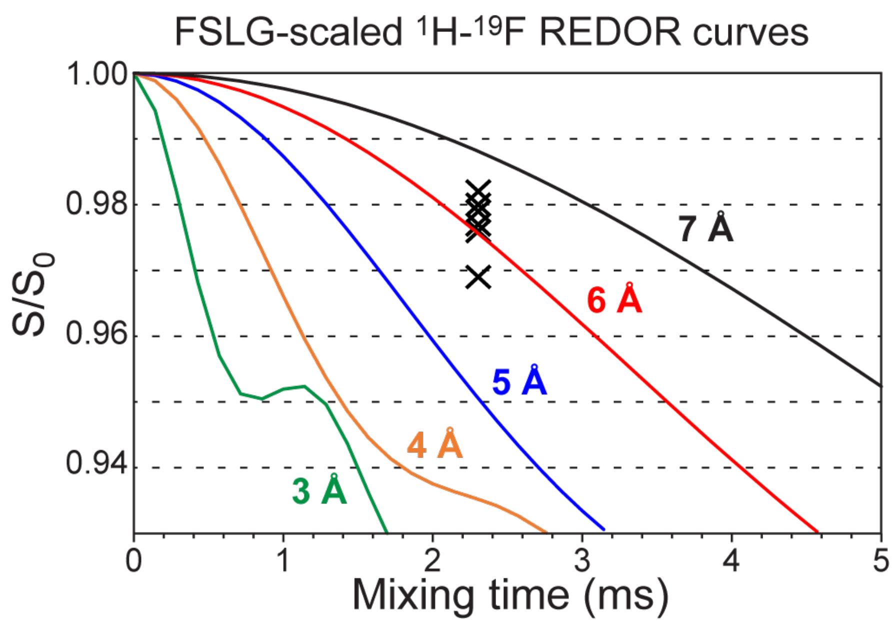

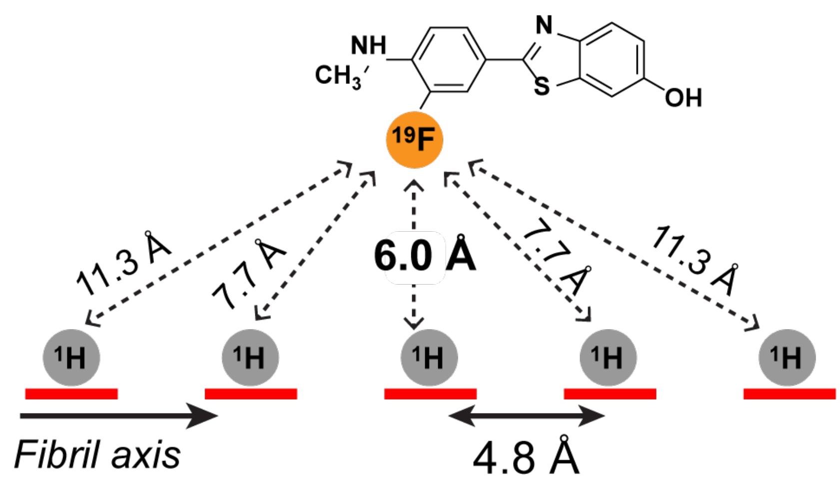

Duan et al. ***J. Am. Chem. Soc.***, 2022.

Conclusions

- Homonuclear and heteronuclear distances can be readily measured in solid-state NMR.
- Homonuclear distances between chemical-shift resolved spins are most easily measured by 2D spin diffusion or dipolar recoupling experiments. Cross-peak intensity buildup can be semi-quantitatively fit to obtain distances.
- Homonuclear distances between spins with the same isotropic chemical shift but different anisotropic chemical shifts can be measured using the CODEX technique and exchange matrix analysis.
- Heteronuclear distances can be measured using dipolar recoupling experiments. The simplest and most robust heteronuclear dipolar recoupling technique is REDOR.
- REDOR can be incorporated into 2D correlation experiments to measure many distances in a single pair of 2D experiments.
- ^{19}F allows distances to be measured to longer range than ^{13}C and ^{15}N.

Acknowledgement

Hong group @ MIT

Alex Shcherbakov

Dr. Matthias Roos

Dr. Pu Duan

Dr. Joao Medeiros-Silva

Venkata Shiva Mandala

Noah Somberg

Dr. Aurelio Dregni

Dr. Matt McKay

Collaborators

Wisconsin Madison: Katie Henzler-Wildman

Wichita State Univ. Haifan Wu

Funding: NIH

HONG LAB

Postdoc positions available.